

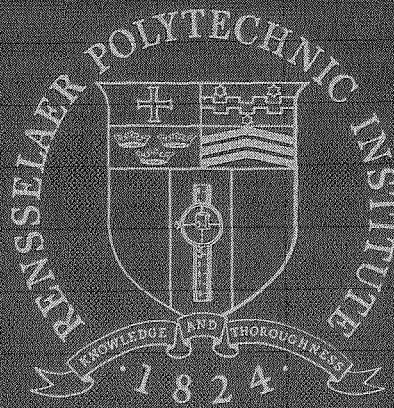
N 70 33990

NASA CR 109797

RPI Technical Report MP-14

TERRAIN MODELING AND PATH SELECTION
IN AN AUTONOMOUS MARTIAN EXPLORATORY
VEHICLE

C. Pavarini and J. H. Chrysler, Jr.



Rensselaer Polytechnic Institute

Troy, New York

N70-33990

RPI Technical Report MP-14

TERRAIN MODELING AND PATH SELECTION BY
AN AUTONOMOUS MARTIAN EXPLORATORY
VEHICLE

C. Pavarini and J. H. Chrysler, Jr.

CASE FILE
COPY

NASA Grant NGL 33-018-091

Analysis and Design of a Capsule Landing System
and Surface Vehicle Control System for
Mars Exploration

JUNE 1970

Rensselaer Polytechnic Institute
Troy, New York

ABSTRACT

The problem considered was the development of the capability of an unmanned Martian exploratory vehicle to safely rove on the surface of the planet. It was required that the vehicle be able to sense the terrain in the direction of travel and choose a safe path toward a distant objective.

The problem of sensing and modeling the terrain was studied in light of sensor capabilities and data processing methods necessary to obtain an accurate approximation to the actual terrain. Improvements were made upon a previously developed modeling technique and computer simulations were carried out on several arbitrary terrains to determine its accuracy. Methods for the evaluation of path-selection algorithms were developed and demonstrated. Heavy consideration was given to the characteristics of the vehicle and the attaining of mission goals.

A path-selection algorithm which takes into account energy requirements in addition to terrain passability and target direction was written. A total package, incorporating the terrain modeling and path selection procedures, was shown to be feasible by computer simulation.

TABLE OF CONTENTS

	Page
ABSTRACT	i
LIST OF ILLUSTRATIONS	iii
LIST OF TABLES	iv
LIST OF SYMBOLS	v
ACKNOWLEDGEMENT	vi
I. INTRODUCTION	1
II. TERRAIN MODELING	2
A. Introduction	2
B. Terrain Definition	4
C. Terrain Data Processing	12
D. Simulation	18
E. Summary	29
III. EVALUATION OF AUTOMATIC PATH-SELECTION ALGORITHMS	30
A. Introduction	30
B. Safety of the Vehicle	32
C. Power and Energy Considerations	43
D. Summary	52
IV. TERRAIN MODELING AND PATH SELECTION INTEGRATION	53
A. Introduction	53
B. 'Cost' Considerations and Interfacing	53
C. A Path Selection Algorithm	60
D. Simulation	61
E. Summary	66
V. CONCLUSIONS	67
REFERENCES	69

LIST OF ILLUSTRATIONS

		Page
FIGURE 1	A Case of Unknown Terrain	5
FIGURE 2	Definition of a Flat Plain	9
FIGURE 3	Possible Terrain Configuration with Flat Plain Data	9
FIGURE 4	Effect of Decreasing $\Delta\beta$ for a Flat Plain	11
FIGURE 5	In-Path Slope Calculation	14
FIGURE 6	Cross-Path Slope Calculation	15
FIGURE 7	Gradient Calculation	17
FIGURE 8	Base Plane for Gradient Calculation	17
FIGURE 9	Flow Diagram for Terrain Model	19
FIGURE 10	Terrain Segment for Simulation 1	21
FIGURE 11	Terrain Model Generation for Simulation 1 .	22
FIGURE 12a	Terrain Segment and Model for Simula- tion 2	24
FIGURE 12b	Sensed Data Points for Simulation 2	25
FIGURE 13	An Azimuth Profile from Simulation 2	26
FIGURE 14	An Azimuth Profile from Simulation 2	28
FIGURE 15	Examples of Trouble-Causing Obstacle Configurations	34
FIGURE 16	Definition of Danger Regions and Levels ...	36
FIGURE 17	Simulation for Average Danger Index	38
FIGURE 18	Possible Positions of Obstacles Between Azimuths	39
FIGURE 19	Possible Positions of the Leading Edge of an Obstacle	41

	Page
FIGURE 20a,b Power ^(a) and Energy ^(b) Requirements for Propulsion of the Vehicle	45
FIGURE 21 A Terrain and Possible Paths	51
FIGURE 22 Batter Energy Drain Per Distance vs. Slope	56
FIGURE 23 Definition of Trade-Off Levels	59
FIGURE 24 Block Diagram of Total Package	63
FIGURE 25 K/k_B vs. Azimuth Path for Total Package Simulation	65

LIST OF TABLES

TABLE 1 Gradient Obstacle Range Location and Errors	20
TABLE 2 Terrain Model Outputs	29
TABLE 3 Data and Calculations for Simulation of Total Package	64

LIST OF SYMBOLS

R	distance from sensor
θ	azimuth angle of sensor
β	elevation angle of sensor
S_I	in-path slope
S_c	cross-path slope
Z_i	relative altitude of terrain point i with respect to the sensor
S_G	gradient
G_{MAX}	maximum slope capabilities of vehicle
ADI	average danger index
RTG	radioactive thermal generator
P	total power requirement of a path
E	total energy expended on a path
D	distance between two terrain points
DTOT	total length of a path
K_B	trade-off level of cost
DT	distance traveled toward target on a path
D_{MAX}	the largest D_T
EBATT	battery drain (in watt-min) along a path
E_c	modified energy cost of a path
E_{MAX}	energy cost of path with target length D_{MAX}
K	calculated cost factor
ROBST	distance from vehicle to obstacle
L	length of a guard band

ACKNOWLEDGMENT

This research was part of a joint faculty-student project at Rensselaer Polytechnic Institute supported by the National Aeronautics and Space Administration. The assistance of students in other design groups was of considerable help in the completion of this study. The authors appreciate the guidance of Messrs. J. Moore and E. Suggs of the Jet Propulsion Laboratory in their roles as technical monitors.

Professor S.W. Yerazunis made many timely and helpful suggestions.

Above all, the authors would like to express their gratitude to Professor D.K. Frederick for his supervision of this research.

I. INTRODUCTION

Under a National Aeronautics and Space Administration Grant, the feasibility of an essentially autonomous Martian exploratory vehicle has been studied. This report concerns itself with analysis and design of the automatic roving capability required of the vehicle. The basic questions involved were; first, what functions were necessary to obtain the roving capability; and second, what were the limiting factors as to how autonomous the vehicle could be? The problem was studied in terms of long-range capability, and the implicit assumption is that there exists some sort of short-range obstacle avoidance system to account for boulders, ditches, and other minor features.

The first requirement is for a line-of-sight electromagnetic sensor that would be able to provide terrain data in the form of angle and range measurements. Then, the sensor data is processed to obtain a usable approximation to the terrain features, denoted as the "terrain model", or "model", for short. Finally, the capability to select a path for vehicle travel, taking into account certain of the vehicle's characteristics is sought.

After a review of past work, the effort was divided into two concurrent studies. The development of a terrain modeling capability was undertaken by Mr. Pavarini. The evaluation of

path selection algorithms, and the implications for the formulation of future algorithms, was studied by Mr. Chrysler. Upon completion of these tasks, a path selection algorithm was written as a joint effort, drawing heavily upon the results in both areas. Then, the interfacing of the terrain modeling and path selection tasks was performed to demonstrate the feasibility of the automatic roving capability total package.

In the following section (II) the work dealing with terrain modeling is presented. Section III relates efforts in path-selection algorithm evaluation, while Section IV contains a new type of selection algorithm and presents a simulation of the entire automatic roving capability package.

II. TERRAIN MODELING

A. Introduction

The terrain modeling function is to create an approximation to the actual terrain ahead of the vehicle in a numerical form which can be processed by the onboard computer. The existence of a discrete, electromagnetic (laser, radar) sensor that is errorless and operates with a vanishingly small beam-width is assumed. The data taken is assumed to be the range (R) to a point on the terrain as a function of the azimuth (θ) and elevation (β) angles. It is desired to use the information contained in these data points to generate a description of those terrain characteristics which will be of importance in selecting

a desirable path. Information is obtainable only at discrete points and the implicit assumption will be made that the terrain is linear between adjacent data points. The model, then, will be a complex polyhedral approximation to the terrain, consisting of planar segments which intersect the actual terrain at their vertices.

It is also assumed that the vehicle will stop at intervals to allow the long-range terrain sensing to occur, and a path to be chosen. The vehicle will then travel to some other point on the known terrain (preferably in the general target direction) and stop again and repeat the process.

Evaluation of any terrain-modeling method poses two main questions:

1. can enough terrain information (data) be obtained to claim that the major features of the terrain are accurately defined by the measurements?
2. does the processing procedure accurately interpret this data (i.e., does the terrain model accurately reflect the actual terrain features)?

Therefore, the study of the terrain model problem centered about the areas of terrain data acquisition and processing. Work was done by Mancini (Ref. 1), who developed several methods of identifying terrain features with the use of a discrete sensor and simple data processing operations. Starting with the most promising of these, the criteria of adequate data

for "definition", and accuracy of the model were applied in an attempt to yield a modeling procedure that would be sufficient for the purpose of long-range terrain modeling and eventually for path selection.

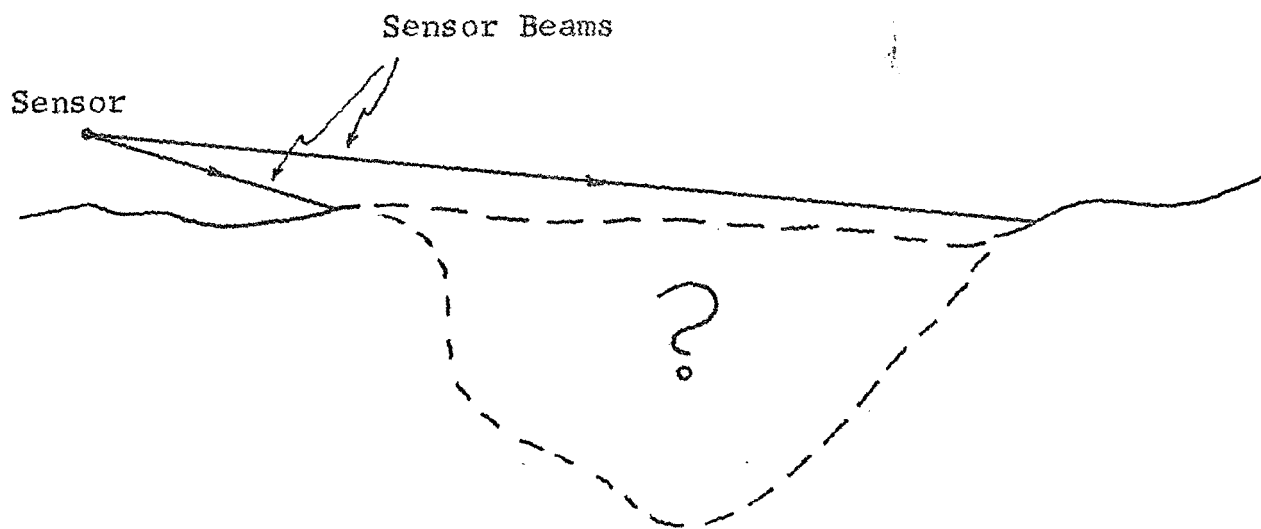
The following sections describe the effort in terrain modeling. First, the question of sufficient data acquisition was examined, resulting in the formulation of necessary sensor parameters. Then attention was turned to the area of data processing techniques sufficient to accurately identify major terrain features. Finally, the behavior of the resultant system was computer-simulated on sample terrains.

B. Terrain Definition

In past work, attempts were made to describe the terrain with the available data, regardless of the location of the data points. However, in the case where data points are separated on the actual terrain by significant distances, the planar approximation to the terrain becomes suspect. In this case, it is invalid to process this data and claim that it is a close approximation to the terrain. Figure 1, for instance, illustrates two possible terrain-profile configurations that would result in the same data input and thus identical models, but would have extremely different implications for vehicle travel.

Consequently, before processing the sensor measurements it must be determined whether or not the terrain data is usable in the sense that it accurately reflects the major terrain

FIGURE 1. A Case of Unknown Terrain



features. A simple test devised for this purpose is to calculate the range differences between adjacent points on the same azimuth line. If any of the differences exceeds a predetermined maximum, it can be said that the data is not likely to be representative of the major features along the profile line. A value for this test maximum was chosen as 300 feet, with the feeling that gross terrain features would be of such a magnitude that they would be "discovered" by data points separated by less than 300 feet. While subject to some real constraints (vehicle size, definition of major feature), this maximum is basically arbitrary, and the actual terrain may or may not behave in the manner supposed. Generally, a 300 ft. maximum made fewer misidentifications than larger test numbers.

To obtain more data points along each azimuth and, as a practical consideration, to increase the angle of incidence of the sensing beam upon the terrain, it is advisable to maximize the height of the sensor above the terrain. With the present vehicle configuration design, it would seem possible to obtain a sensor height of perhaps ten feet. This height was assumed throughout the study.

The important thing to realize is that sensor height should be maximized, consistent with structural considerations, e.g. rigidity, weight. With a constant $\Delta\beta$, the realizable maximum range for adequate definition increases linearly with sensor

height. In addition, the effective range of the sensor itself would most likely be increased with sensor height due to the improved impingement angle.

Since the thrust of this work is in long-range modeling, distances of interest were chosen to be those in excess of 200 feet from the sensor location. In addition, it is desired to extend the maximum range of the model in order to minimize the number of sensing stops the vehicle will be required to make in order to travel some total distance. Of course, the limits on maximum range will depend on the electromagnetic sensor's range limitation, but the limits will also be functions of both type of terrain and other sensor capabilities (especially elevation angle increment). As distance from the sensor location is increased, distance between adjacent data points also increases if $\Delta\beta$ is constant. If, past a certain data point, all these differences exceed 300', the process is unable to "define" terrain past a point which is at a distance closer than the sensor's maximum range.

Elion (Ref. 2) indicates that laser technology gives, as a rule of thumb, beam divergences of 10^{-3} radian without optics, and notes that figures of 2×10^{-4} radian have been achieved. Carroll (Ref. 3) implies that experimentation in the early sixties resulted in beamwidths of 4×10^{-6} radian, by the use of collimating optics.

As a starting assumption, then, the elevation angle increment ($\Delta\beta$) was set at 5 milliradians (0.286 degree). It was found

that with this order Δ/β , and using the 300' identification test, a realizable range maximum on most terrains is somewhat less than 2000 ft.

All parameter choices were developed from examination of data acquisition on various postulated terrain segments, and thus, these values are vaguely suspect from the start. Choice of terrain types used in analysis was guided by knowledge about the Martian surface (Ref. 4,5). Therefore, due to the number and types of terrains utilized, and their similarity to current best estimates of Martian terrain, a fair amount of confidence can be placed at least on the order of magnitude of these parameters.

The most vexing problem to come out of this analysis was the realization that the easiest terrains to "define" were those which were least well suited to vehicle travel. Smooth, slightly-sloping terrains consistently failed the acquisition test because a sufficiently close set of points was not obtainable along terrain profile lines. However, for steeper slopes and highly contoured regions the data points are well placed. Typically, for a sensor height of ten feet and an evaluation angle increment of 5 milliradians, gently sloping terrain (the most ideal traveling path) was impossible to "identify".

Figure 2 shows the data acquired along one azimuth line of a perfectly flat plain. Applying the sufficient definition test it is found that there is no portion of the terrain that

FIGURE 2. Definition of a Flat Plain

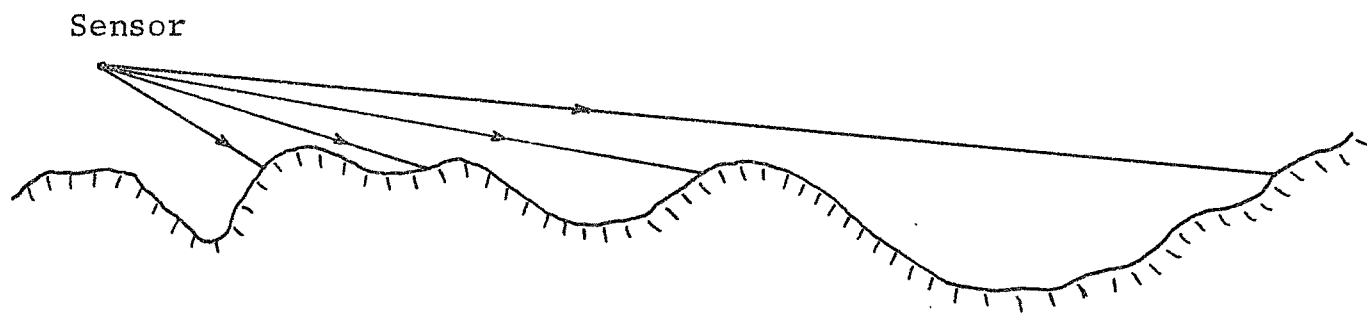
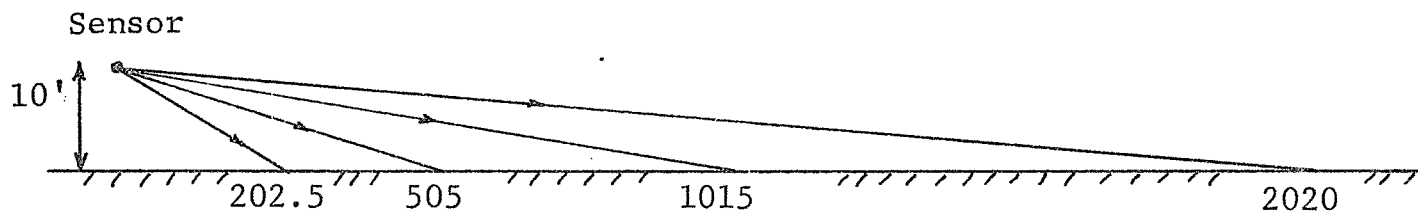


FIGURE 3. Possible Terrain Configuration with Flat Plain Data

can be claimed to have been defined. It is entirely possible that the actual terrain could be as shown in Fig. 3 and yet the terrain data from an ideal sensor would be identical to that obtained on the flat plain.

In order to define the terrain in this simple but important case, it was necessary to use a smaller elevation angle increment. The choice was made to decrease $\Delta\beta$ to 5/3 milliradian, but only in the cases where the smaller $\Delta\beta$ is required, namely, where the sufficient data test has been failed. In some cases, e.g., easy to define terrain, $\Delta\beta = 5$ mr is satisfactory: however, in those cases where data points are widely spread along a profile, the smaller $\Delta\beta$ is required. Figure 4 demonstrates the additional data obtained in the case of sighting on a flat plain with the smaller elevation angle increment. The plain is now "defined".

If the elevation angle increment were to become infinitely small, there would remain cases where sufficient data could not be obtained. This would occur when large portions of the terrain were out of the line-of-sight of the sensor. Thus, there is no justification for decreasing $\Delta\beta$ indefinitely. On terrains where there is insufficient data, there is not enough information to make any claims about the terrain between the data points. While an obstacle has not been detected, there is nothing to indicate that the region is obstacle free. In this

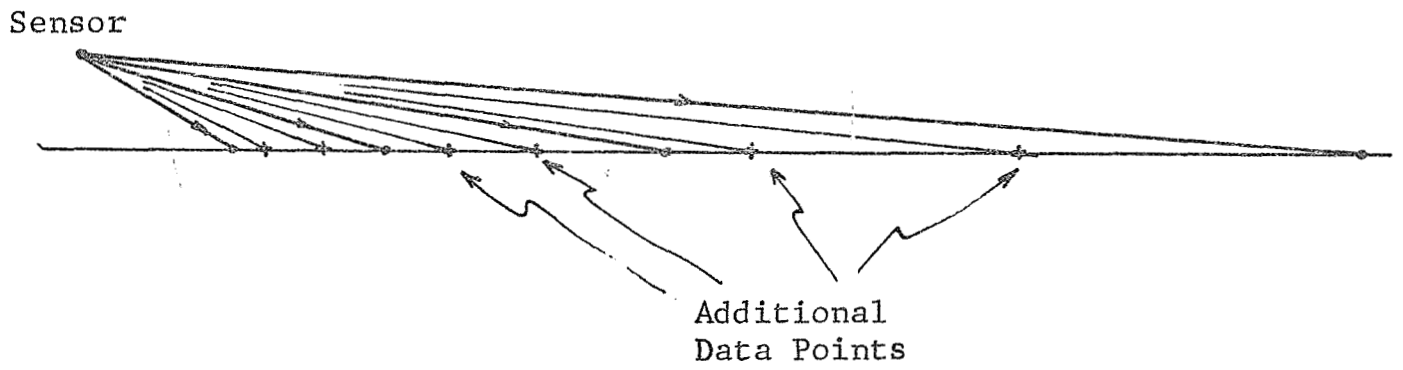


FIGURE 4. Effect of Decreasing $\Delta\beta$ for a Flat Plain

case, the only legitimate output of the terrain modeling process would be, without further operation, to declare a hidden or unknown region to exist at that location. This designation is one of the possible outputs of the terrain model.

In essence, an attempt was made to find those sensor parameters which, within practical limitations, would allow the best definition of the terrain viewed by the sensor. There remain cases where sufficient data is not available for definition, and these cases preclude further analysis of these areas.

C. Terrain Data Processing

Given that on some portion of the terrain segment of interest, there is an area sufficiently defined to allow major feature approximations to be made, obtaining an accurate representation of the actual terrain is the next task. As concern is ultimately for vehicle travel on some portion of this terrain, and since the primary obstacles to the vehicle will be steep slopes, the most desirable information would be some indication of the slope of the region around each data point. This information will be contained in a number called the gradient, where gradient will be defined as the line of steepest slope through the data point in the approximating plane formed by the adjacent data points.

To obtain the gradient, two intermediate calculations will be made:

- 1) In-path slope (S_I) - the slope of the line joining adjacent points along a constant

azimuth line.

- 2) Cross-path slope (S_C) - slope of a line perpendicular to the azimuth line, and in the plane of the terrain approximation.

Reference 1 demonstrates a method for calculating the gradient using four data points, two points on each of two adjacent azimuth lines. It will be shown that similar results can be obtained using a three-point method which has the advantages of simplicity, smaller storage requirement and less computer time. Referring to Figure 5, it can be shown (Ref. 1) that

$$S_x = \frac{R_2 \sin \beta_2 - R_1 \sin \beta_1}{R_2 \cos \beta_2 - R_1 \cos \beta_1}$$

For a sensor height of ten feet and ranges between 200 and 2000 feet, the elevation angle of the sensor (β), the horizontal being $\beta = 0$, will be very small, allowing small-angle approximations to be employed, such that

$$S_x \doteq \frac{R_2 \beta_2 - R_1 \beta_1}{R_2 - R_1}$$

The cross-path slope is calculated in order to eventually describe the gradient of a three-point planar approximation to the terrain. Figure 6a shows a top view of two adjacent azimuth lines, with $\Delta \theta$ being the angle between these azimuth lines. P_1 , P_2 , and P_3 are real points, that is, they are data

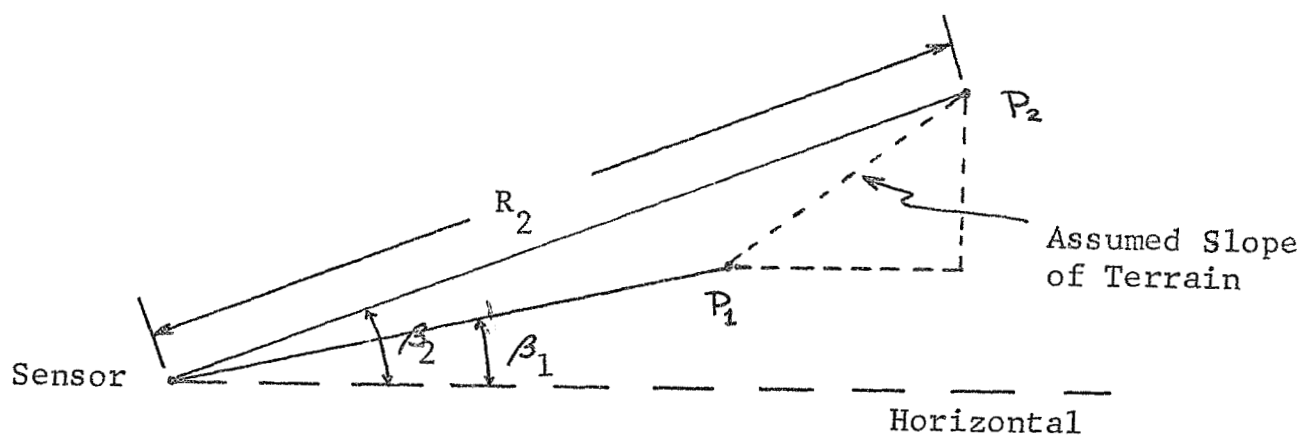


FIGURE 5. In-Path Slope Calculation

Top View

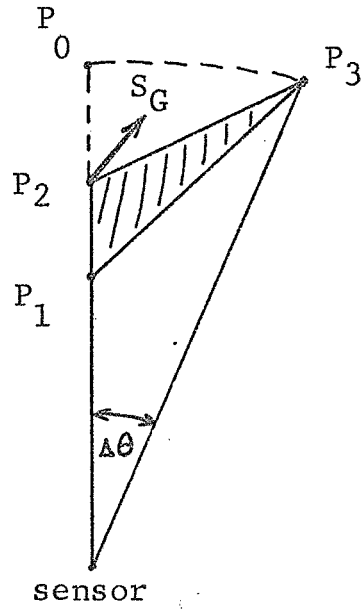


FIGURE 6a. Cross-Path Slope Calculation

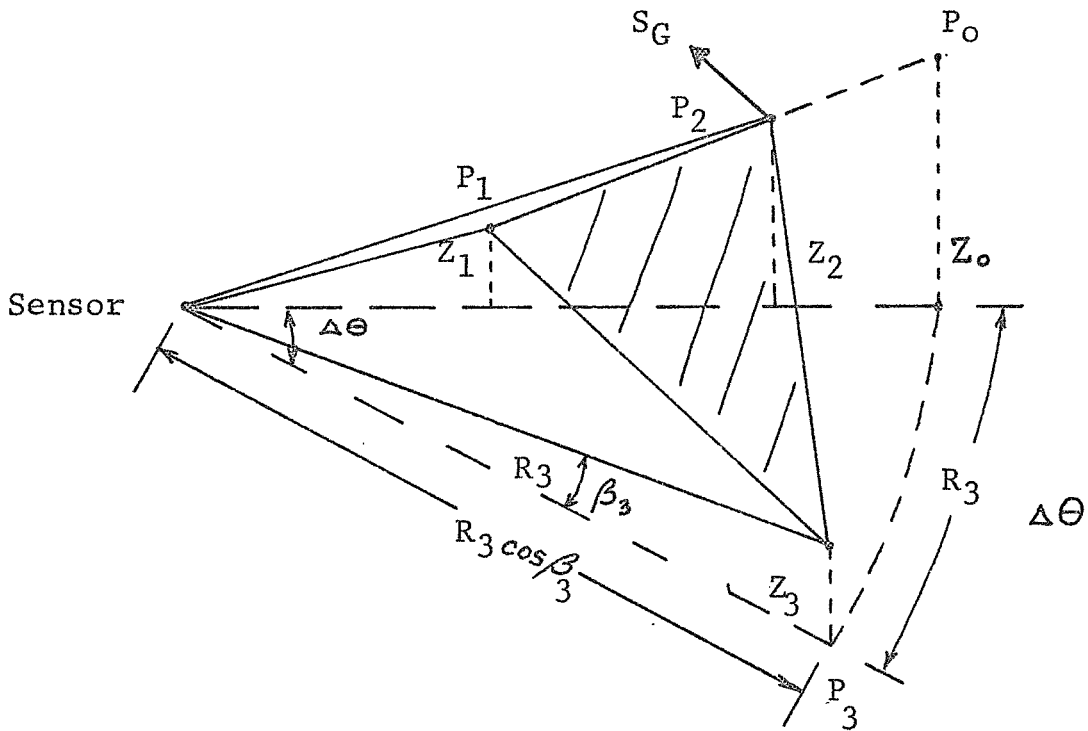


FIGURE 6b.

points representing a sensing beam impingement on actual terrain. The gradient at point 2 is to be calculated. P_0 is a projected point used solely for computational purposes. As can be seen in Figure 6b, P_0 is the intersection of a cylindrical surface (with a radius $R_3 \cos \beta_3$ and major axis which is the vertical line through the sensor position) and the line of slope S_I through P_1 and P_2 . The height of the three data points (Z) is, to a good approximation:

$$Z_i \doteq R_i \beta_i \quad i = 1, 2, 3$$

Letting

$$\Delta R_0 = R_3 - R_2$$

then

$$Z_0 \doteq Z_2 + S_I \cdot \Delta R_0$$

Finally,

$$S_c \doteq \frac{Z_0 - Z_3}{R_3 \cdot \Delta \theta}$$

Having calculated S_I and S_c , a fictitious plane can be created having the same gradient as the terrain approximation plane. This is shown in Fig. 7. If we denote the gradient by S_G , then

$$S_G = \frac{H}{L}$$

Figure 8 is a top view of the base of Fig. 7. From Fig. 8, it follows that

$$\sin \alpha = \frac{1/S_c}{\sqrt{\left(\frac{1}{S_c}\right)^2 + \left(\frac{1}{S_I}\right)^2}}$$

Also

$$\sin \alpha = \frac{L}{H/S_I}$$

then

$$S_G = \frac{H}{L} = \frac{S_I}{\sin \alpha} = \sqrt{(S_I)^2 + (S_c)^2}$$

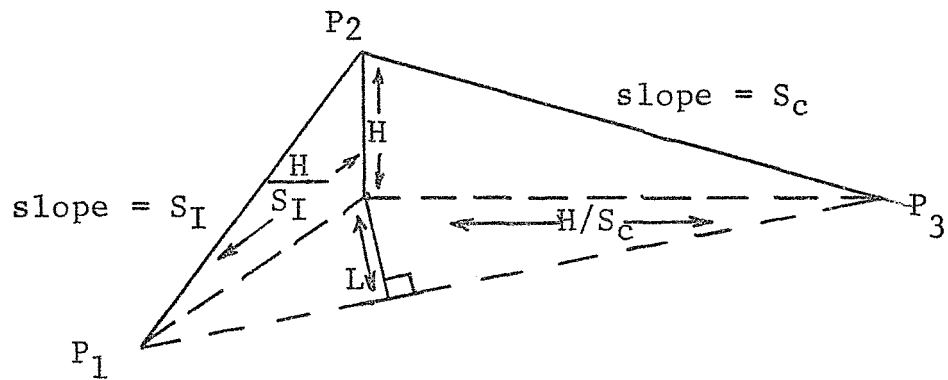


FIGURE 7. Gradient Calculation

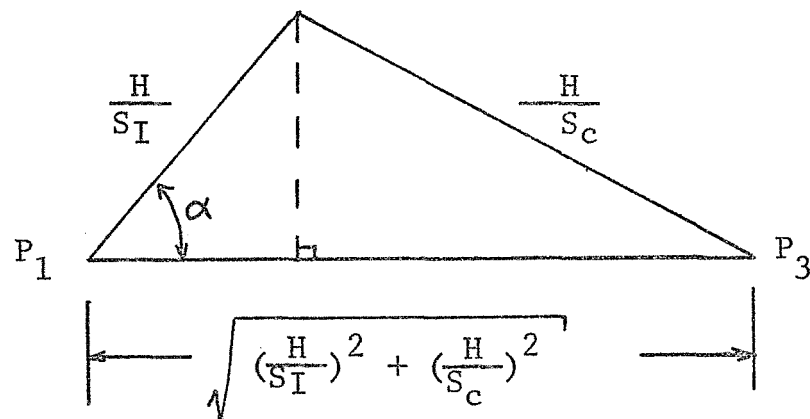


FIGURE 8. Base Plane for Gradient Calculation

The ability to calculate the gradient allows the definition of a second type of region on the terrain model. Due to both its geometry and power limitations, the vehicle will be limited to the maximum slope it can traverse (G_{\max}). Thus, comparing the calculated value of S_G with the known G_{\max} will allow the labeling of each point of the terrain as to its suitability for travel. Those portions of the terrain where $S_G > G_{\max}$ will be identified as gradient or slope obstacles, the second possible output of the terrain modeling procedure.

Calculations are done along each azimuth line from points of smallest to largest range. If, along any azimuth, there are no unknown regions, and no gradient obstacles, there will necessarily be a point of maximum range, due either to the sensors's range being exceeded, or the terrain being totally hidden beyond this point. The lack of terrain information beyond this point precludes any statement as to the suitability of this area for travel. This presents the third possible output of the modeling process, namely, the indication that the terrain is passable along the azimuth line up to a point of maximum range of the sensor. Figure 9 is a flow chart for the terrain modeling calculations. In the next section, the quality of the model will be tested by simulation on sample terrains.

D. Simulation

The first terrain used for simulation was a 90°

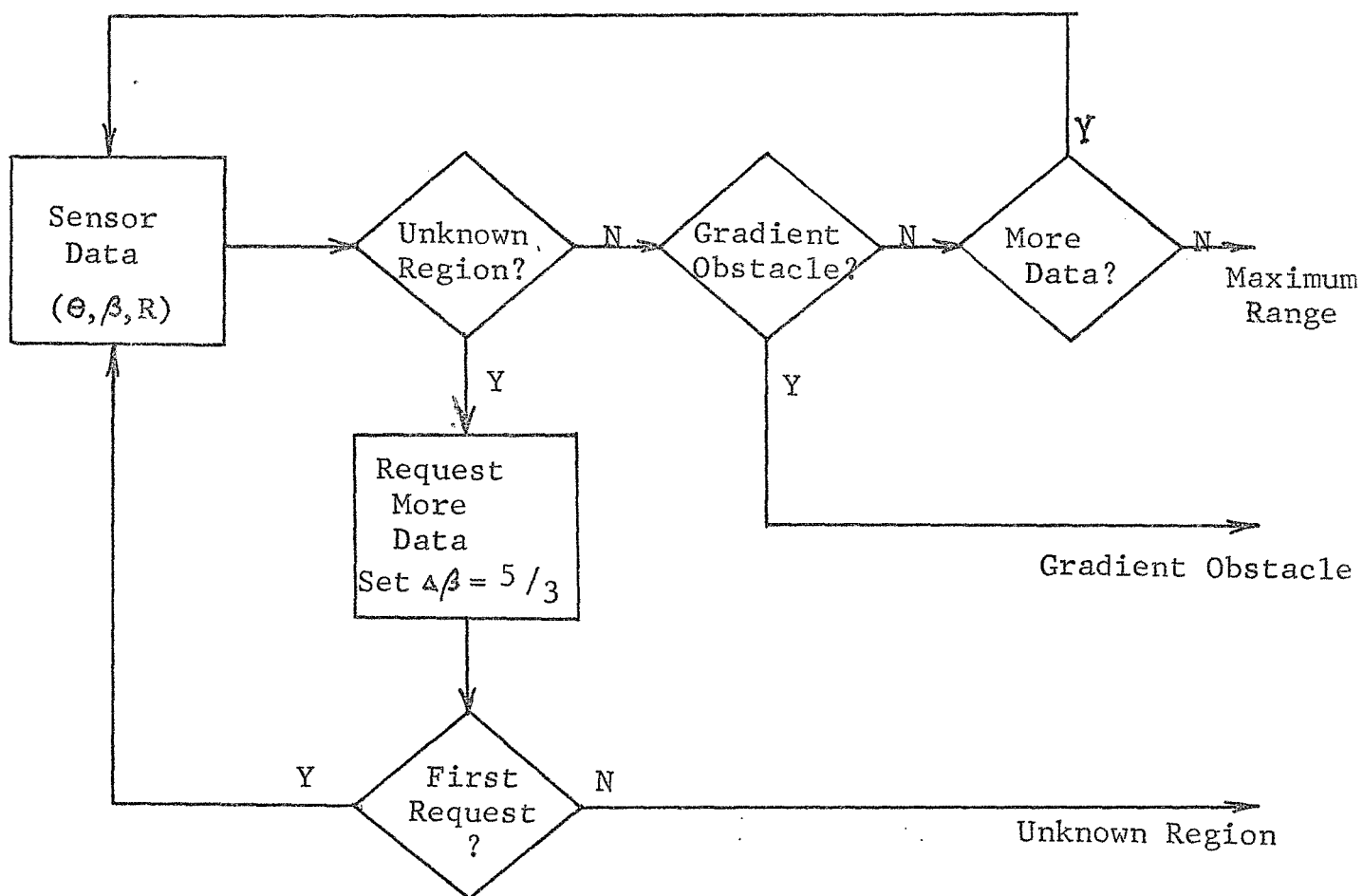


FIGURE 9. Terrain Data Processing Calculations

pie-slice, which was created so as to be easily defined.

Figure 10 shows a contour map of this region along with an outline of the actual gradient obstacle region. In this case, the maximum sensor range was chosen as 1600 feet, the azimuth angle increment ($\Delta\theta$) as 5° , and the maximum allowable gradient (G_{max}) was assumed to be 10° .

Figure 11 indicates the obstacles modeled by the process for each azimuth superimposed upon the actual obstacle region. Note that maximum range obstacles do not necessarily occur at the exact maximum range of the sensor. For those azimuths passing through the obstacle region, Table 1 summarizes the accuracy of the model as an approximation of the actual terrain.

TABLE 1
GRADIENT OBSTACLE RANGE LOCATION

Azimuth	actual	model	error	% error	Over-Estimate ROBST?
-5°	1015	1000	+15	1.5	No
0°	1115	1110	+ 5	0.5	No
5°	1100	1130	-30	2.7	Yes
10°	1090	1060	+30	2.8	No
15°	1160	1220	-60	5.2	Yes
20°	1260	1310	-50	4.0	Yes

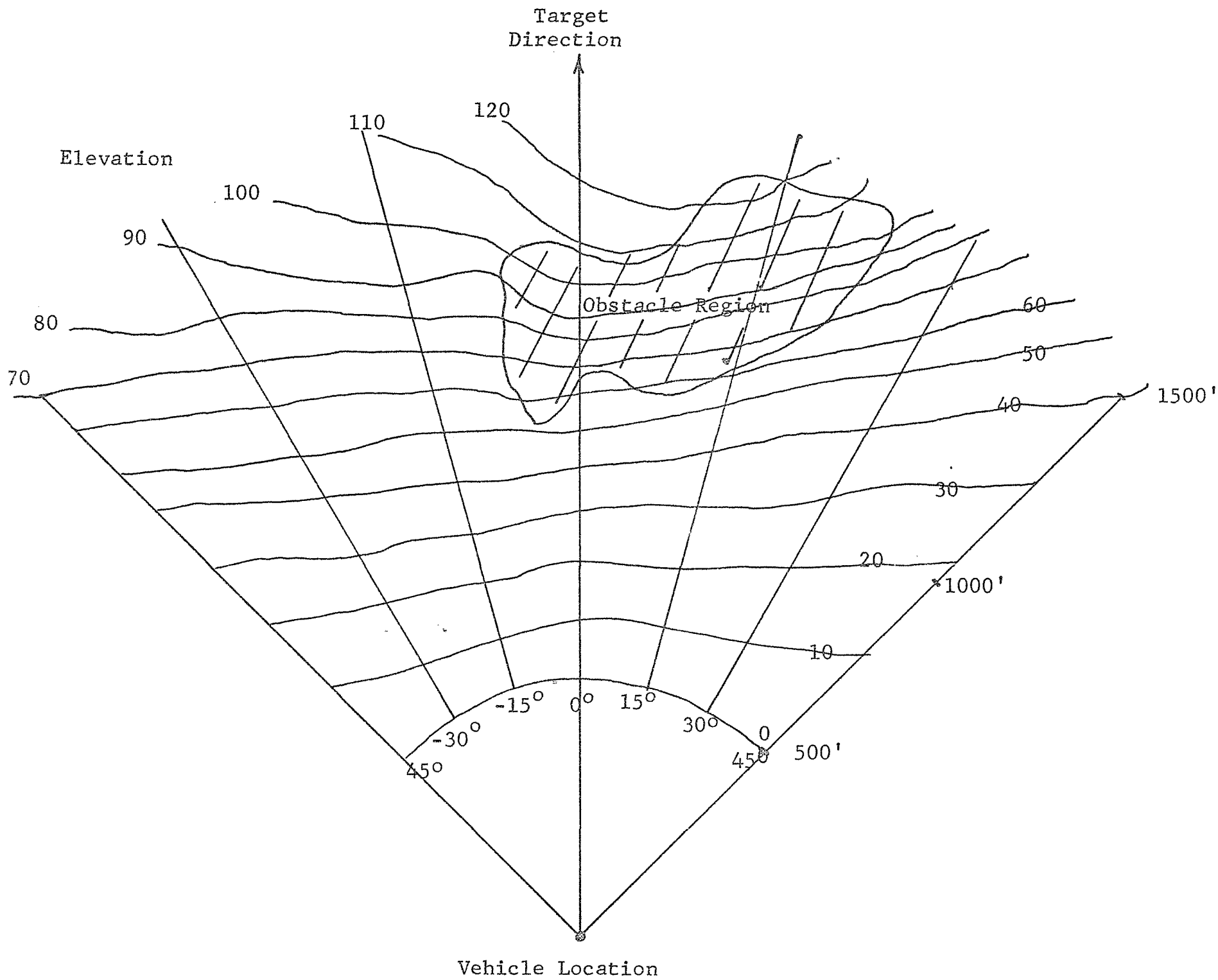


FIGURE 10. Terrain Segment for Simulation 1

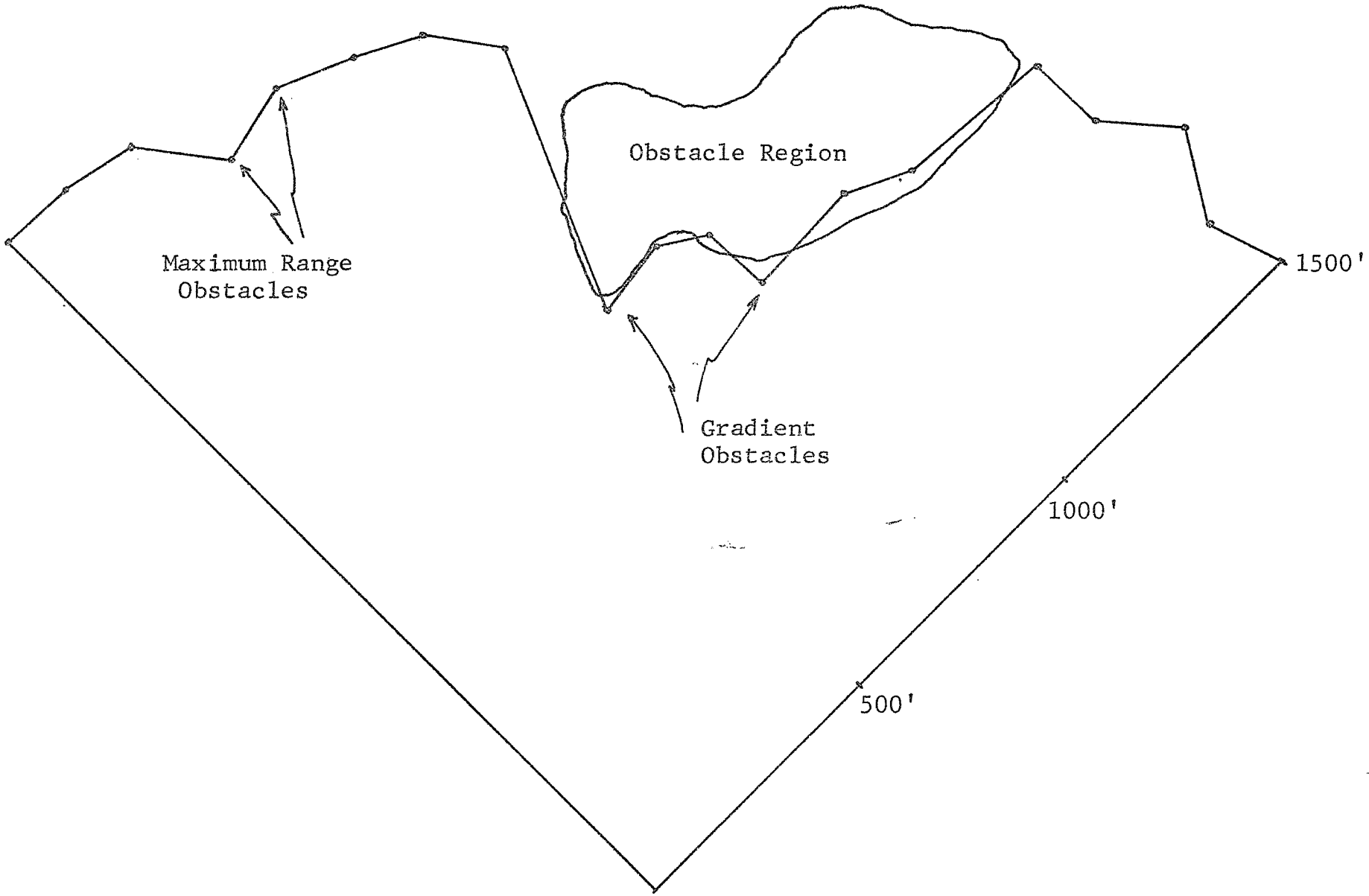


FIGURE 11. Terrain Model Generation for Simulation 1

Note that there were no hidden regions, due in part to the fact that slope generally increases with the distance from the sensor. There were no areas of gradient obstacles that the model was unable to identify. In addition, general slopes of other areas on the terrain were closely approximated.

As a further test of the modeling process, a second terrain was formulated with the specific intention that it be a difficult type to model. Figure 12a is a contour map of the 60° pie-slice used. Superimposed are gradient obstacle regions (cross-hatched). Figure 12b shows the sensed data for some azimuths.

Those points sensed with a 5 milliradian elevation angle increment scan are shown as dots, while the additional data points obtained by decreasing $\Delta\beta$ to 5/3 milliradian are denoted by crosses. In addition to being gently sloping, the terrain contained hidden regions and gradient obstacles of varied orientation (S_I, S_C), and was of sufficient range to enable examination of a reasonable maximum defining range.

A profile sketch (with an expanded vertical scale) of azimuth (-20°), (Fig. 13) illustrates the case of a hidden or unknown region. The downslope occurring in the 600-1300 foot range was untouched by the sensing scan at $\Delta\beta = 5$ mr, while reducing the value $\Delta\beta$ to 5/3 mr (dotted lines) served only to narrow the gap by 100 feet. All of the terrain between 770 feet and 1440 feet along this particular azimuth is completely hidden; that is, it is out of the line-of-sight of sensing beams.

FIGURE 12a. Terrain Segment for Simulation 2

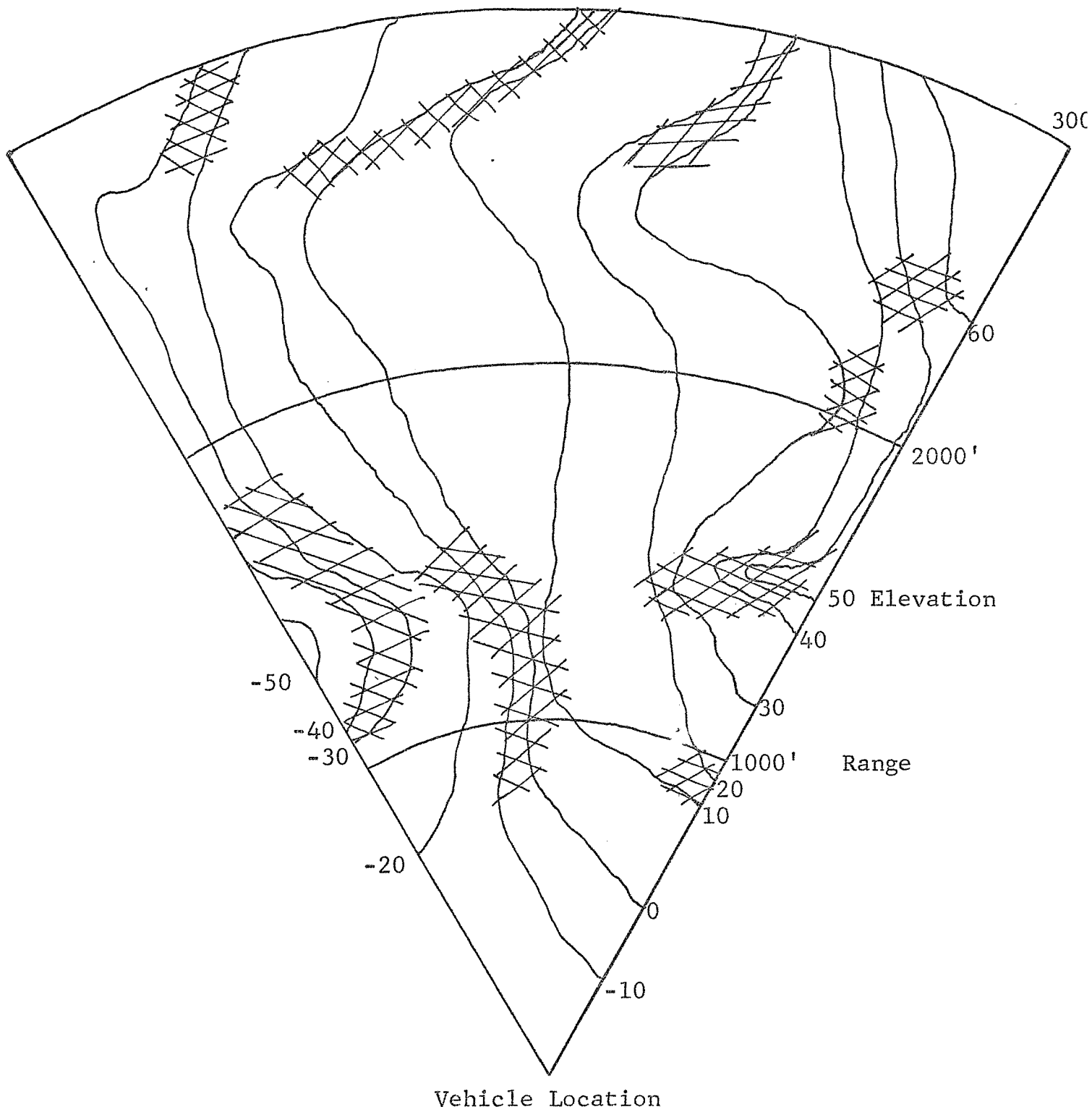


FIGURE 12b. Sensed Data Pts. for Simulation 2

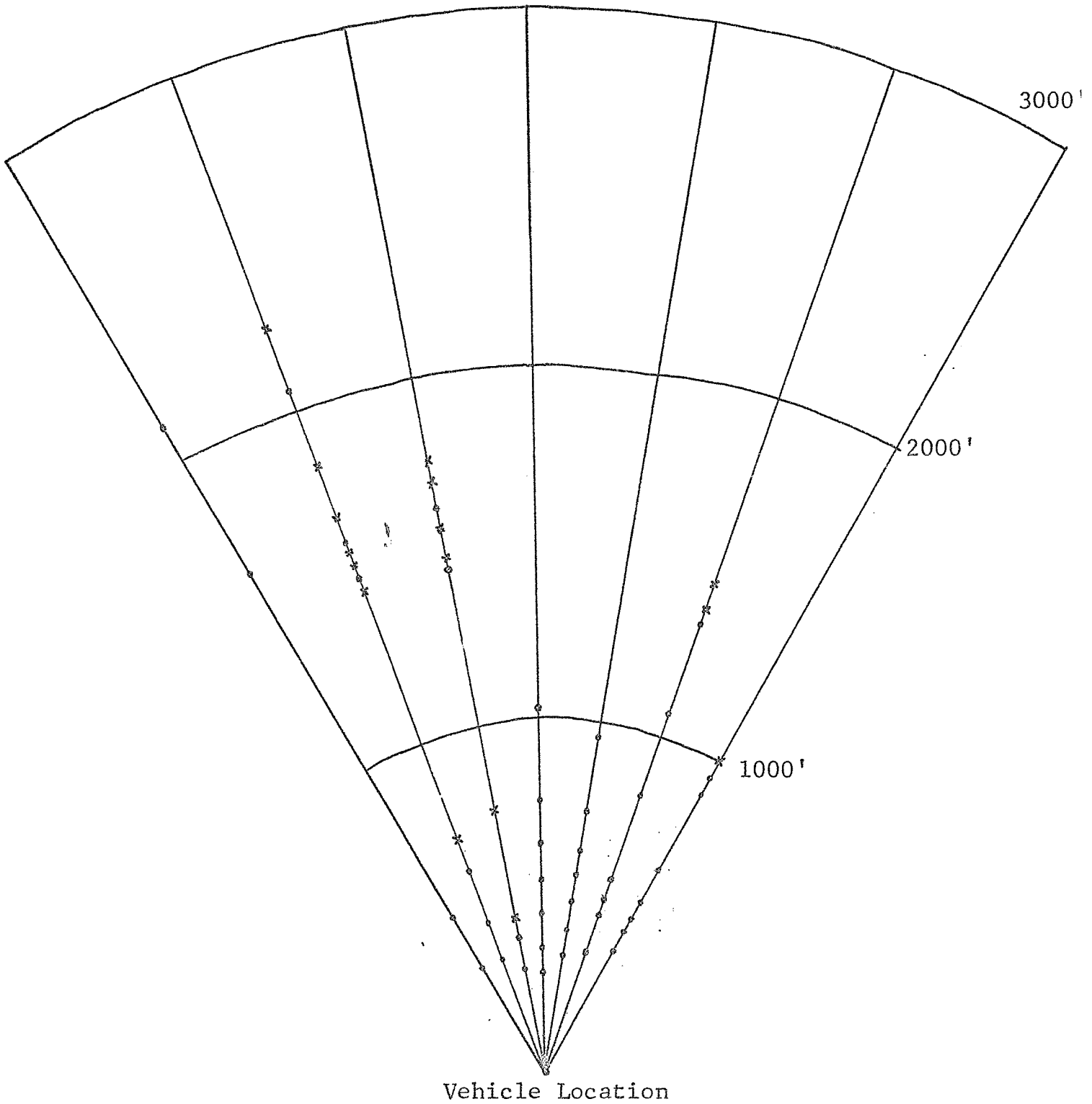
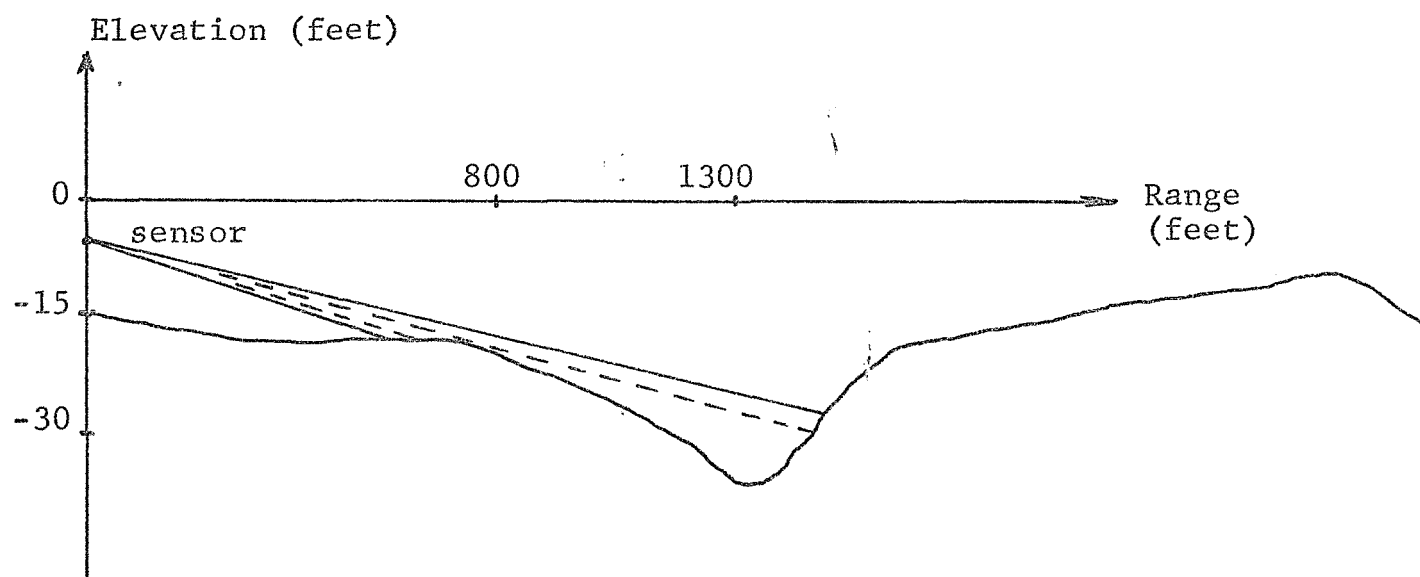


FIGURE 13. An Azimuth Profile from Simulation 2



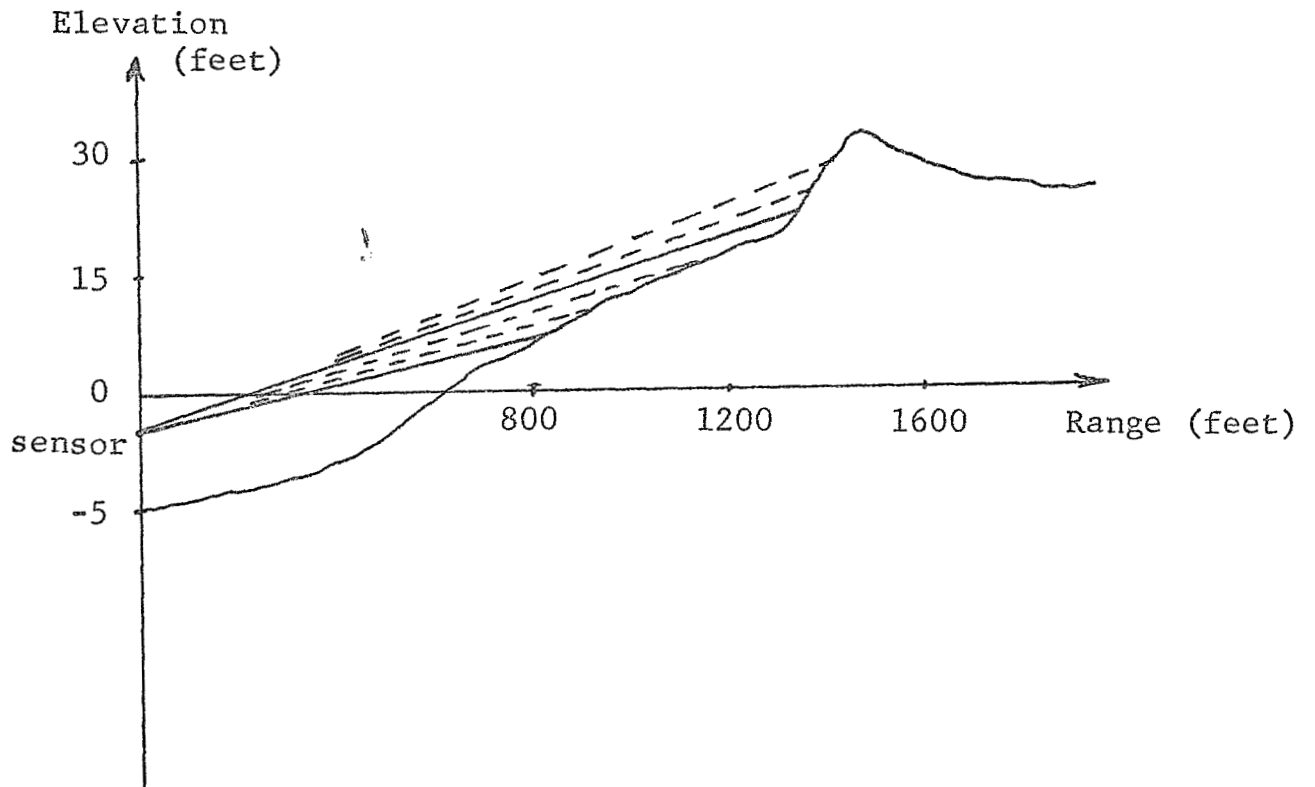
Azimuth (+15°) (Fig. 14) is a case of an unknown region being defined by additional sensing. Noteworthy are the maximum range obstacle at 1380 feet and the extremely small angles of incidence for all data points in excess of 850 feet. Also, maximum range is increased by 70 feet by going to the smaller Δ/β .

On this terrain, continuous identification of terrain along an azimuth was largest for azimuth (20°) the value being 1480 feet. In most cases, either unknown or maximum-range obstacles occurred in the 500-1000 foot range, terminating adequate data acquisition at those ranges. Generally, data was sparse for ranges in excess of 1800 feet.

All of the major terrain features that occurred on the near side of unknown regions, and within sensor range, were identified. (In-path slope obstacles to within 30' with no over-estimation of range to obstacle). However, the definition of cross-path obstacles was less exact (± 70 ft). This was due in part to the dependence upon a good match between the ranges on both azimuths to localize the approximation (refer to gradient calculation derivation).

Because there are an infinite number of terrains the sensor might be called upon to model, simulation is certainly not a proof of the infallibility of the modeling procedure. Computer simulations were run in order to examine the behavior of the method under "operating" conditions, to find acceptable

FIGURE 14. An Azimuth Profile from Simulation 2



values for the sensing parameters ($\Delta\theta$, $\Delta\beta$, and sensor range), and to search for any situations that might not have been considered in formulation of the process. While it is realized that the results are necessarily biased by individual terrain choices as well as by sensing parameters, the identifications made on a total of 32 azimuths tested are summarized in Table 2.

TABLE 2
Terrain Model Outputs

obstacle	gradient	unknown	max. range
number	10	7	15
average range	1120	730	1330

E. Summary

A terrain modeling capability requires that adequate data be available to identify the terrain. After determining a test for sufficient data acquisition, it was possible to identify the sensor parameters necessary for terrain definition.

Once the possible outputs of a terrain modeling process were identified, data processing techniques that resulted in a model which closely approximates major terrain features were derived and simulated on sample terrains.

In addition to the above results, a most important output of the terrain modeling work is the effect of a terrain modeling procedure upon determining evaluation criteria for path-selection algorithms. The knowledge of what the outputs of the

model are, and to what extent they can be trusted, is necessary before one can decide if the way an algorithm treats these outputs is correct or in any way optimum. This dependency will be apparent in the following section.

III. EVALUATION OF AUTOMATIC PATH-SELECTION ALGORITHMS

A. Introduction

The final step in the operation of the automatic roving capability of an unmanned Martian vehicle is that of automatic path selection. An algorithm must be available to use the information from the terrain modeling process and select a path that will lead the vehicle toward the target. The path-selection process should also consider the important limitations on the overall system imposed by the mission requirements and by the actual design of the vehicle.

Past work in the area of automatic path-selection algorithms, both by Lallman (Ref. 6) and Lim (Ref. 7) has been primarily concerned with the formulation and testing of various algorithms. These past algorithms have had the common characteristics of being essentially two dimensional in make up. They used a terrain map that had only two types of regions, namely, free and obstacle types, or "go" and "no-go". The no-go regions were areas in which the terrain modeling process found a gradient obstacle and this is the only three-dimensional information that the path-selection algorithms used. There

was no differentiation between slopes in the free regions.

These algorithms were concerned with the sole problem of finding a path through a sample terrain to a given target. The selection process did include the important idea of maximizing the distance traveled toward the target when considering the various possible paths.

Because it is possible to devise a great variety of path-selection algorithms, it becomes increasingly important to have a quantitative means for evaluating different algorithms. The first step was to look at the overall system and determine what parameters were important. The selection of these parameters is dependent upon both the mission requirements and the actual vehicle design.

Once the important parameters were identified, a performance index was formulated that was related to each area of concern. Each index assigns a quantitative measure to the performance of a given algorithm on a sample terrain. The quantitative nature of the index then allows the comparison of different algorithms, on the same terrain, to determine which does the best job.

The problem of evaluating algorithms is quite similar to the study that should go into the formulation of new algorithms. Therefore, the utility of the work on path-selection algorithm evaluation in the writing of future algorithms would appear to be an important by product of the study. These implications are

discussed in each of the two major areas of concern. These ideas have been put to use in the formulation of a new type of path-selection algorithm and in the integration of the terrain modeling and path-selection algorithm tasks, both of which will be discussed in Section IV.

B. Safety of the Vehicle

A mission to put an unmanned roving vehicle on the surface of Mars will necessarily have to place a high priority on the success of that mission. In relation to automatic path selection, this means that algorithms must be available that will select a path that will keep the vehicle clear of terrain hazards. For example, it would be better for a path-selection algorithm to fail in finding a path rather than to send the vehicle on a path that would be considered too dangerous. If such a difficult terrain confronted the vehicle, the control should be switched to Earth where visual pictures could be used to help guide the vehicle. An alternative to this might be the adaptation of the path-selection algorithm to reflect the type of terrain in which the vehicle is operating. Either way, a path-selection algorithm should be quite conservative with respect to the safety of the vehicle when choosing a path.

For the purpose of evaluating algorithms with respect to the safety of the vehicle, an Average Danger Index (ADI) has been formulated. It is a heuristic performance index that assigns

a quantitative measure to how close the path selected by a path-selection algorithm lies to the obstacles in the terrain.

$$ADI = \frac{\sum_{\text{all regions}} (\text{danger level})^2 \times (\text{path length})}{\text{total path length}}$$

To use the average danger index a sample terrain or terrain model is selected. For the algorithms now in existence, this would be a two-dimensional terrain map with go and no-go regions marked off on it. The no-go regions correspond to the gradient obstacle and unknown regions discussed in the previous section. Contours are then drawn about the obstacle regions and assigned a danger level. The danger level would naturally increase as the obstacle is approached. Because of this, it is desirable to have a path-selection algorithm that would keep the vehicle a reasonable distance from obstacles. This is the type of performance that the average danger index is designed to measure.

Once a sample terrain has been selected, the regions drawn, and the danger levels assigned, the average danger index can be found for any given path on that terrain using the above formula. A set of rather simple terrains could then be used to test how various path-selection algorithms react to obstacle configurations that are known to cause trouble.

Some of the obstacle configurations that are known to cause trouble are shown in Figures 15a-c. Each figure shows a

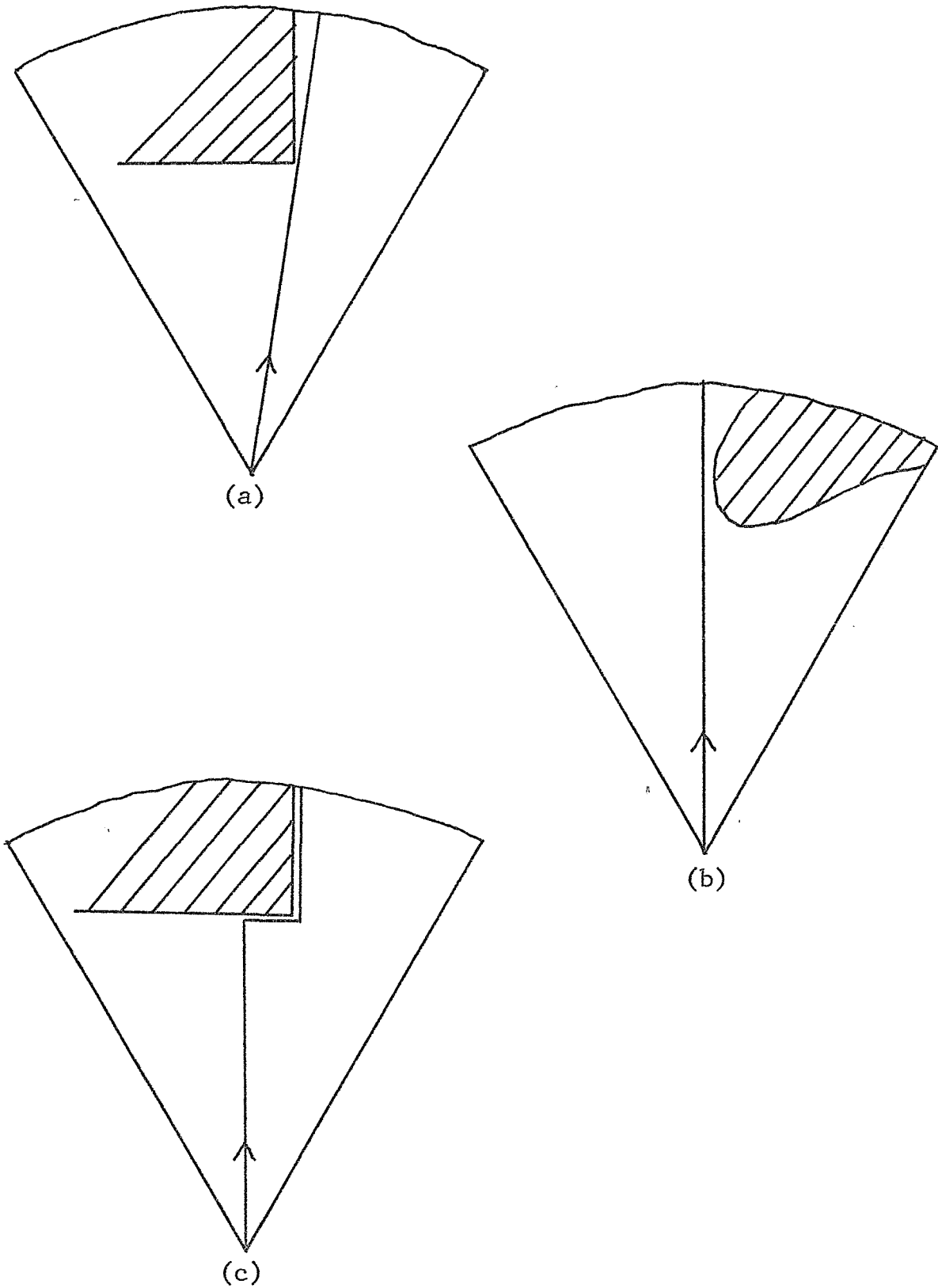


FIGURE 15. Examples of Trouble-causing Obstacle Configurations.

different way in which path-selection algorithms have chosen paths that would lead the vehicle dangerously close to an obstacle. These characteristics can be classified as cutting corners too closely^(a), traveling too close when passing an obstacle^(b) and approaching too close before detouring around an obstacle^(c).

The average danger index can be used to test either the path-selection algorithms or the complete terrain modeling and path-selection algorithm package. The latter of these two applications should prove to be of the greatest value. The ability to test the terrain modeling and path selection units together is important because the safety of the vehicle is not only dependent on the path-selection algorithm but on the accuracy of the terrain modeling process that is being used.

Example

A simple example will illustrate the use of the ADI. For this simulation, a two dimensional terrain map was used to evaluate variations of one of Lallman's algorithms. The overall width of the danger region was taken to be 100 feet. This was then subdivided and the regions were assigned danger levels according to the graph in Fig. 16. This definition was used in order to put a greater penalty on crossing from an 8 region to a 10 region than from a 4 to a 6 region by narrowing the width of the regions as the danger increases. This is consistent with the

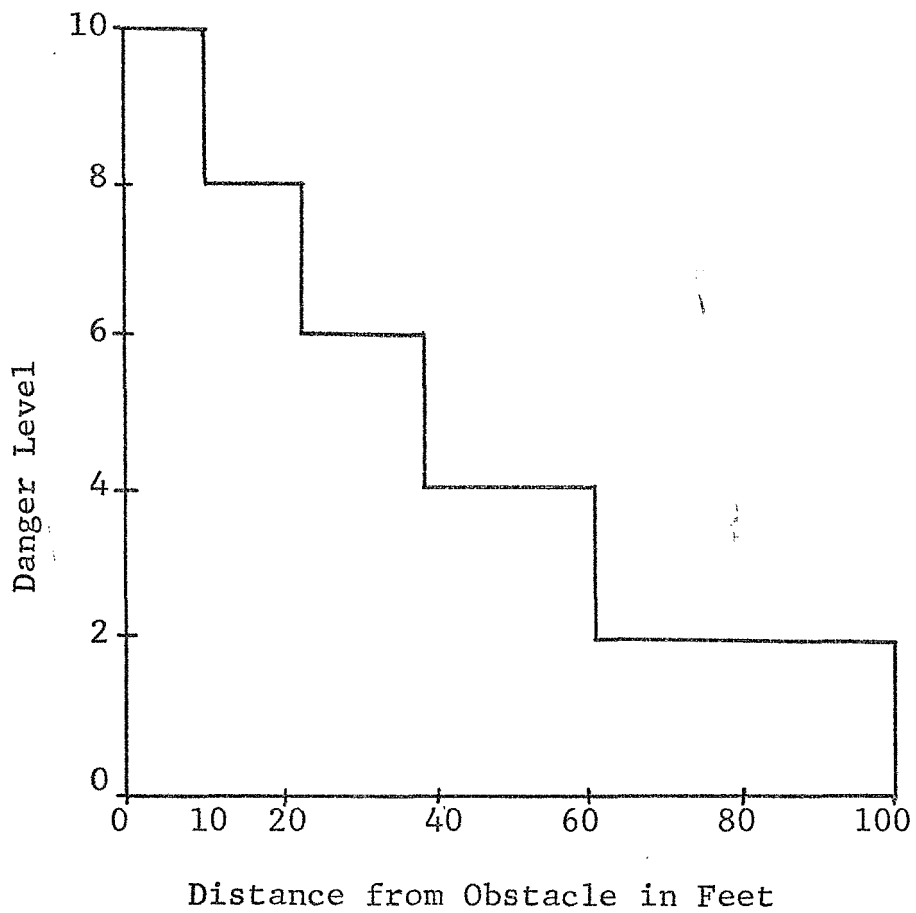


FIGURE 16. Definition of Danger Regions and Levels

high concern for the safety of the vehicle.

The sample terrain and results of the simulation are shown in Fig. 17. The average danger index for paths 1, 2, and 3 are approximately 48, 4, and 0 respectively. This indicates that path 3 is safer than path 2, which is in turn safer than path 1. It also indicates that the algorithm that selected path 3 would be the most desirable of the three. This algorithm keeps the vehicle completely out of the danger region while only losing 30 ft. in the distance traveled toward the target compared to the most dangerous, and longest path.

Implications for Future Path-Selection Algorithms

Under the proper circumstances each of the algorithms tested exhibited the very dangerous characteristic of traveling arbitrarily close to an obstacle. This occurred either while approaching or passing an obstacle. To realize just how serious this problem can be it is necessary to take a close look at the actual terrain modeling process.

If a gradient obstacle or unknown region is found along a given azimuth and not along the adjacent azimuth, it is known that the obstacle must end somewhere in between. The problem is that the actual placement of the obstacle in that region is not known and it could lie arbitrarily close to the azimuth that was labeled as free, as indicated Fig. 18. In choosing any particular azimuth, the long-range path-selection package

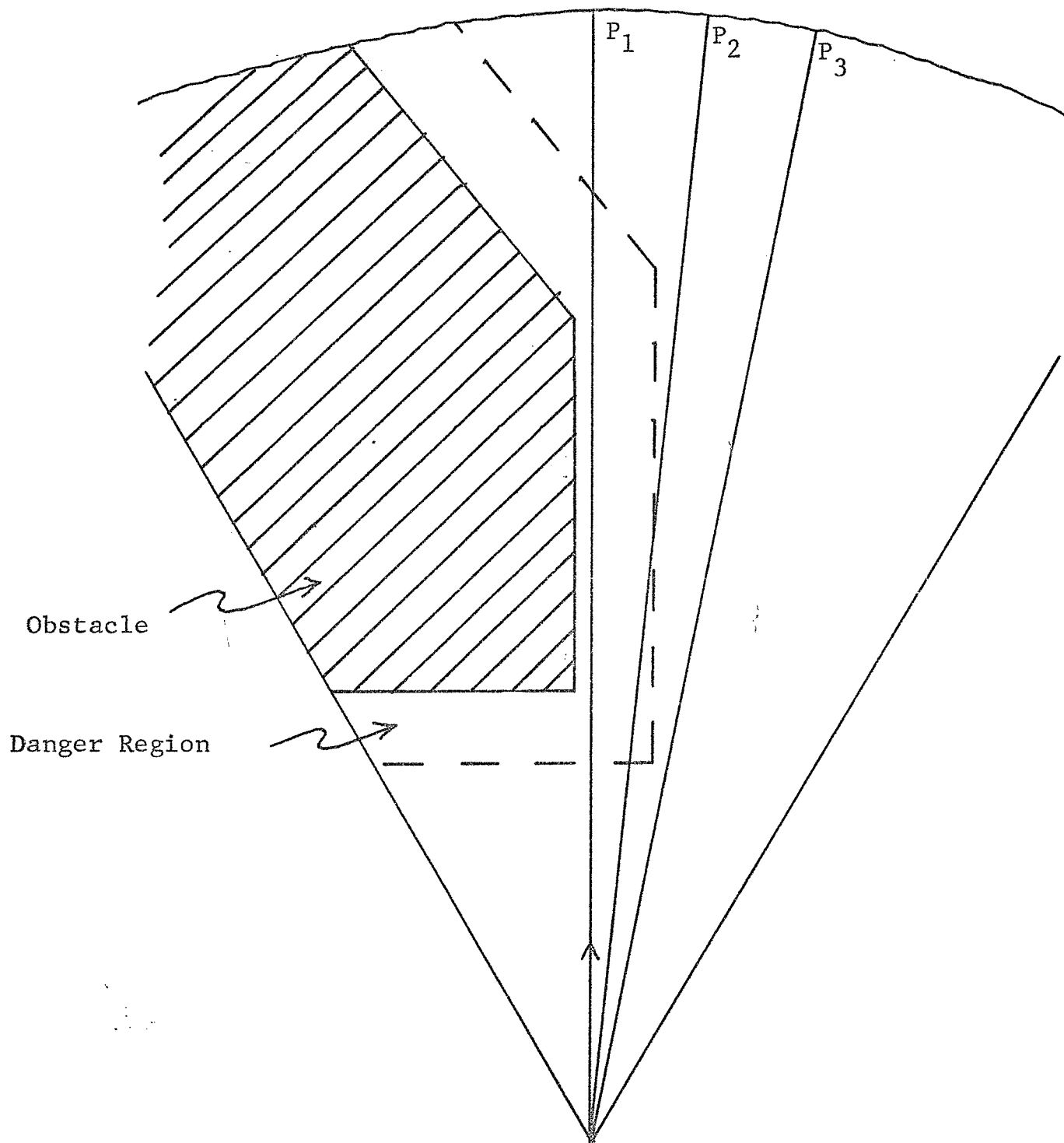
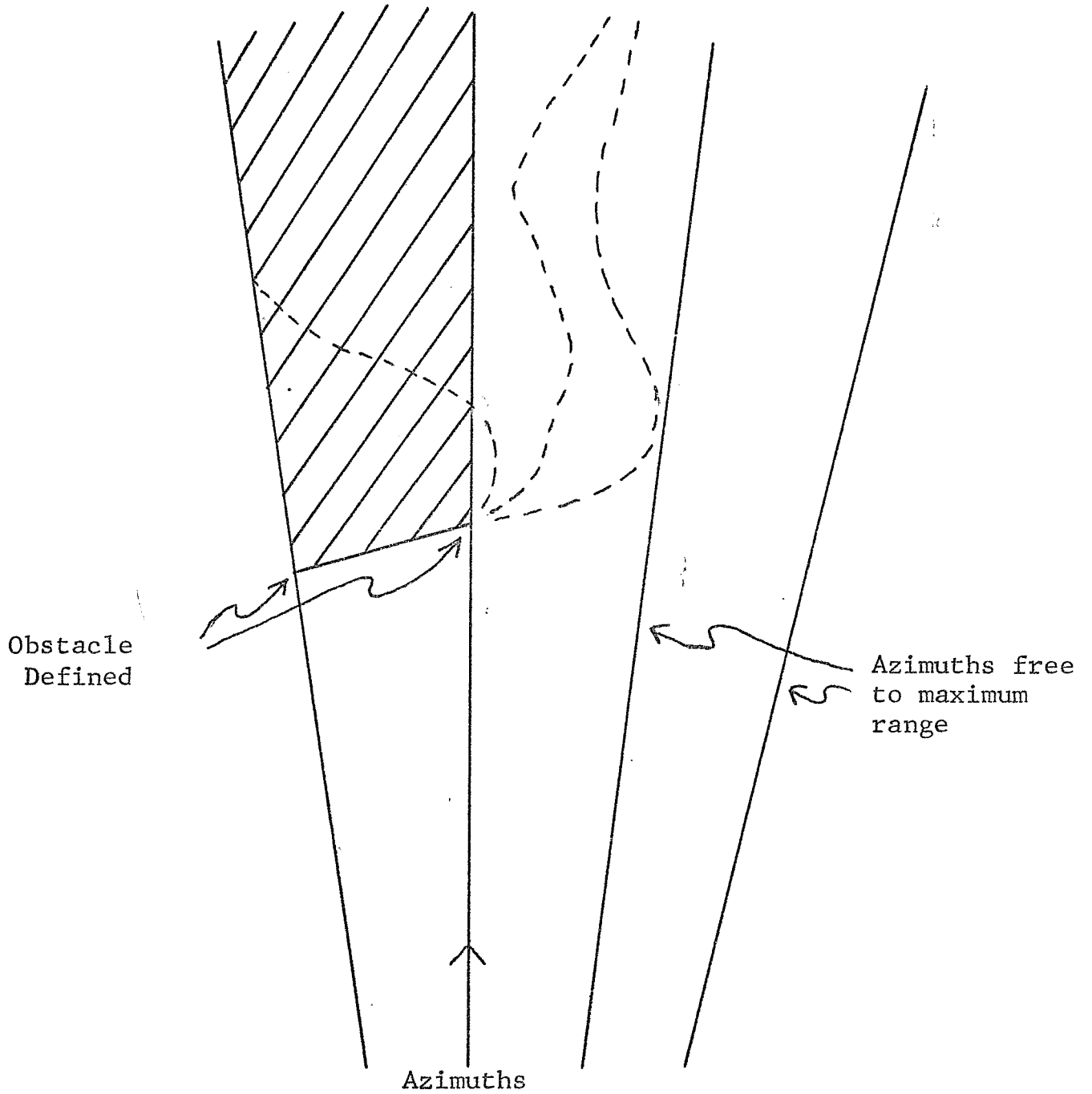


FIGURE 17. Simulation for Average Danger Index

FIGURE 18. Possible Positions of Obstacles Between Azimuths (indicated by dashed lines).



is just picking a general direction for the vehicle to travel. It is expected that the vehicle will wander somewhat from the selected azimuth as the short-range obstacle-detection system guides the vehicle around small terrain hazards. In light of this, the vehicle should not be allowed to travel along any azimuth that would lead it next to a gradient obstacle or unknown region.

Perhaps the path-selection algorithm should not consider any azimuth that is adjacent to one that ends at a gradient obstacle or unknown region. Or if such an azimuth is to be considered, it should not be considered past the point where the obstacle was defined on the adjacent azimuth. This procedure would keep the vehicle from traveling arbitrarily close to an obstacle region as it proceeded to travel around that obstacle.

In traveling directly up to an obstacle the same sort of problem exists. In reference to Fig. 19, if either a gradient obstacle or unknown region is found along an azimuth at point 8, the actual leading edge of that obstacle is somewhere between points 7 and 8. Again, the actual position is not known and it may lie arbitrarily close to the point 7. For reasons of safety, guard bands should be placed on the leading edges of the obstacles defined by the terrain modeling process. The guard bands are meant to restrict the travel of the vehicle to less than the total distance to an obstacle before it stops

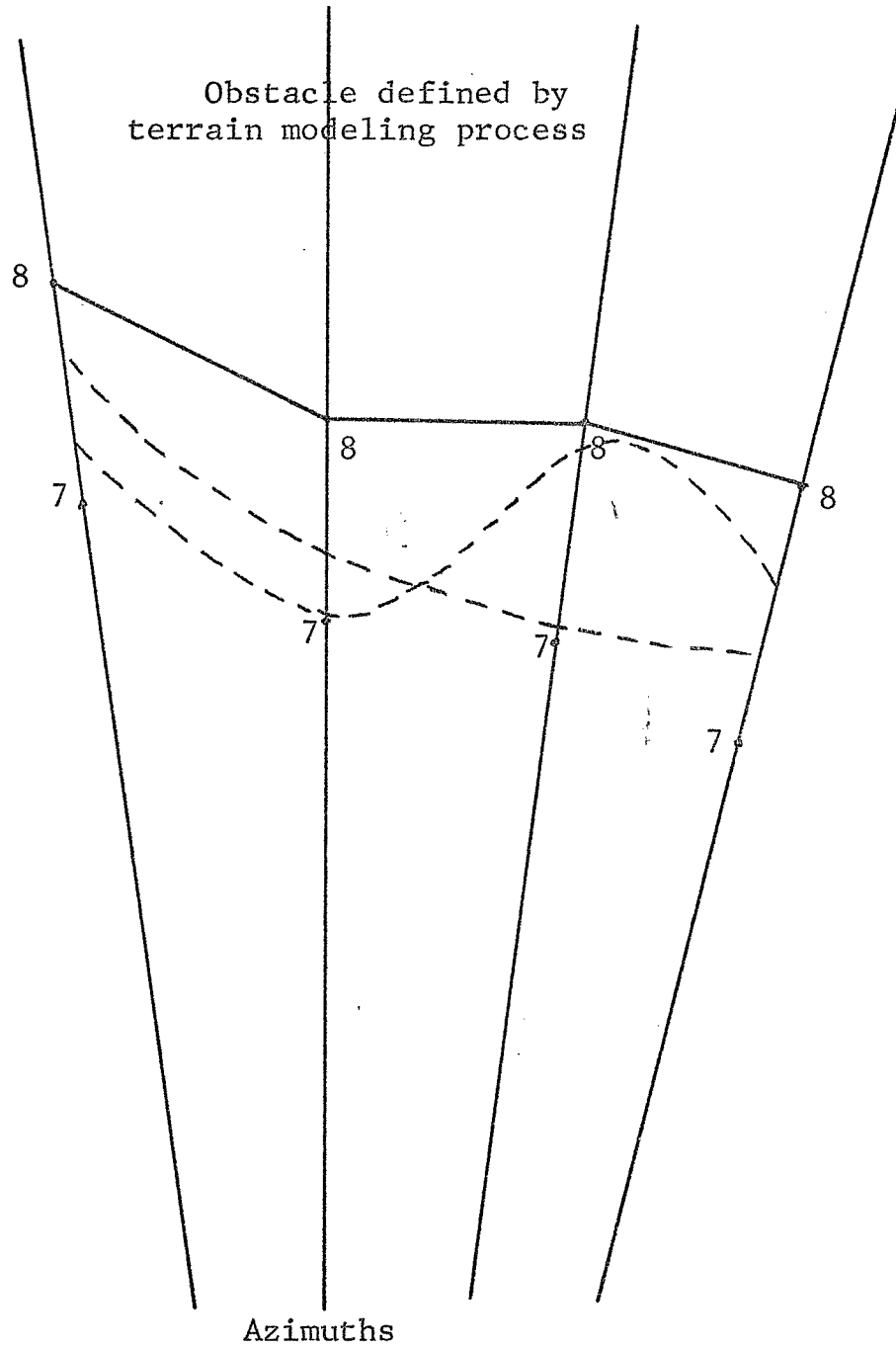


FIGURE 19. Possible Positions of the Leading Edge of an Obstacle (indicated by dashed lines).

to acquire new data.

The size of the guard bands should be a function of the distance from the vehicle to the obstacle. Or equivalently, a function of the distance between the data points. The size of the guard bands should increase with the distance from the vehicle because the data points to which they are related are spread farther apart as the distance increases. Also, errors in the sensor would have a greater affect on the terrain definition as the distance increases, since it has been shown that the distance between data points increases with distance from the vehicle.

The size of the guard bands at any given range should also be dependent on the type of obstacle that is defined. The gradient obstacle should have the largest guard band in front of it as it is known that trouble lies within that region. It is quite easy for passable terrain to be defined as an unknown region; therefore, this type of obstacle should have a smaller guard band associated with it. The out-of-range obstacle is one that is clear terrain to a certain point. This type of obstacle should naturally have the smallest guard band. In varying the size of the guard bands in this way, they are being used to penalize the travel towards one type of obstacle more than another. This is done in a manner that is consistent with the high concern for safety.

One area that needs to be looked into in some detail in the future is the possibility of an adaptive navigation system. The path-selection and/or terrain modeling processes could be modified to reflect the general type of terrain that the vehicle is traveling in. For example, if the terrain was fairly free of gradient obstacles, the paths that would lead to that type of obstacle might be dropped from consideration. The guard bands on the other types of obstacles might be able to be decreased also. In particularly rugged terrain, the opposite would be true. The guard bands would have to be increased and paths leading towards gradient might have to be considered because they might be the only ones available.

The terrain modeling process could also be modified. The present process defines anything over 10 degrees as a gradient obstacle. This value could be changed to reflect the general type of terrain the vehicle was traveling in. These modifications could be made either automatically or from the Earth control center.

C. Power and Energy Considerations

The second area of major importance is that of the power and energy required by the vehicle. This area is affected by both the mission requirements and the vehicle design. Some of the factors that are related to the path-selection task are: the total distance the vehicle is to travel, the desired

speed, the amount and weight of the power supplies, and the power used by the vehicle. It is not the purpose of this report to delve deeply into the power and energy requirements and make-up of the vehicle. Much of the information concerning this area was obtained from the vehicle design group at RPI.

Discussion with members of the vehicle design group has indicated that power and energy requirements pose strong limitations on the vehicle. It is very important to minimize the power and energy required for the operation of the vehicle.

For the roving capability, the majority of the power used by the vehicle is likely to be for propulsion. The amount used for steering, data processing equipment, etc., is comparatively small. Power and energy curves can be derived from potential energy considerations, using a 2 degree slope as level ground to account for frictional losses. Graphs for power vs. slope and energy per distance vs. slope are shown in Figs. 20a and b. These graphs are for a constant vehicle speed and an Earth weight of 1000 lbs. Their derivation will be shown in Section IV.

The importance of power and energy would indicate that a path-selection algorithm should use this type of information when selecting a path. Therefore, a performance index has been formulated to evaluate different algorithms as to how well they minimize the amount of energy used by the vehicle.

Before a performance index could be selected, it was necessary to take a closer look at the actual power make up of

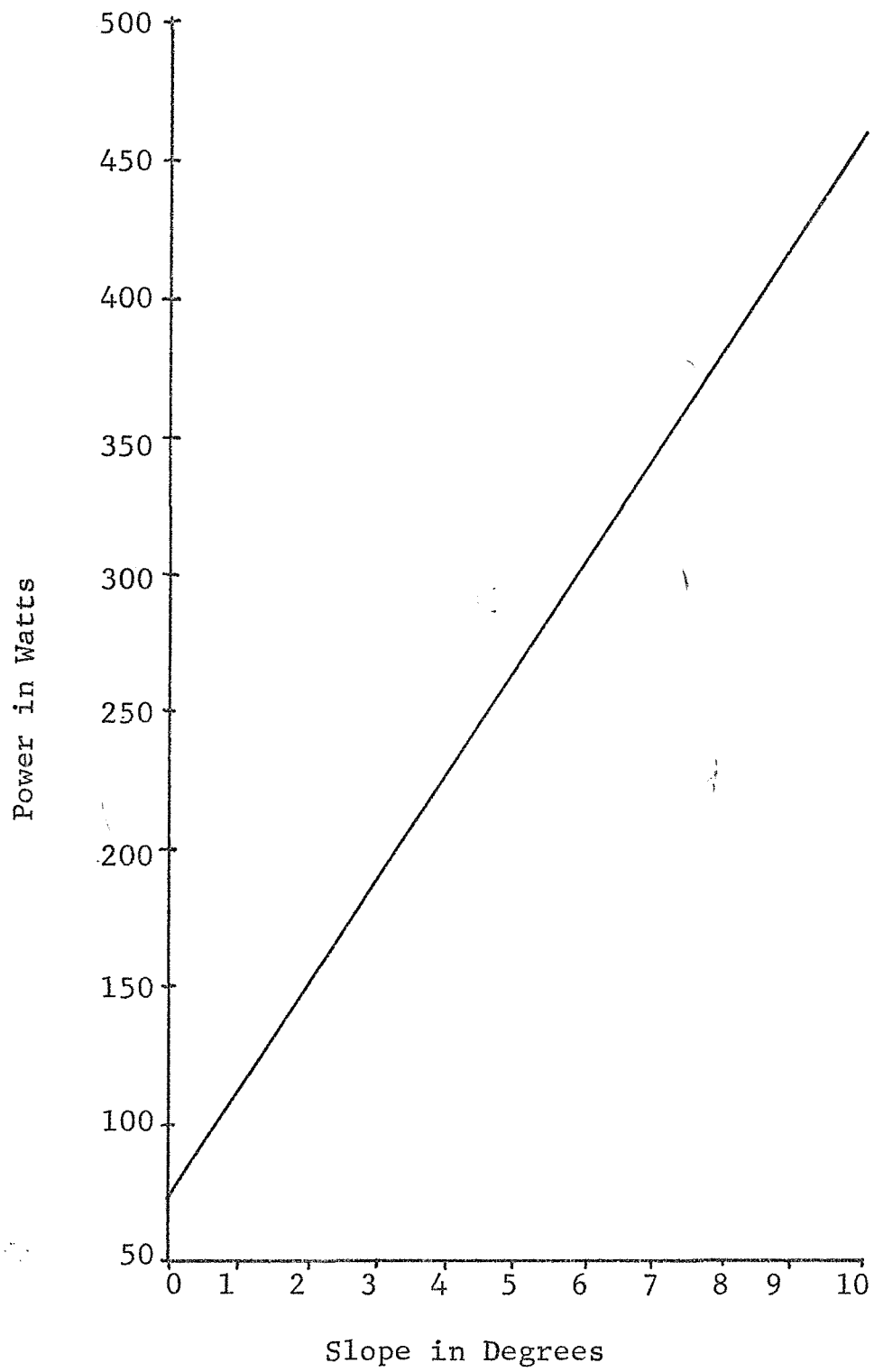


FIGURE 20a. Power Requirements for Propulsion of the Vehicle.

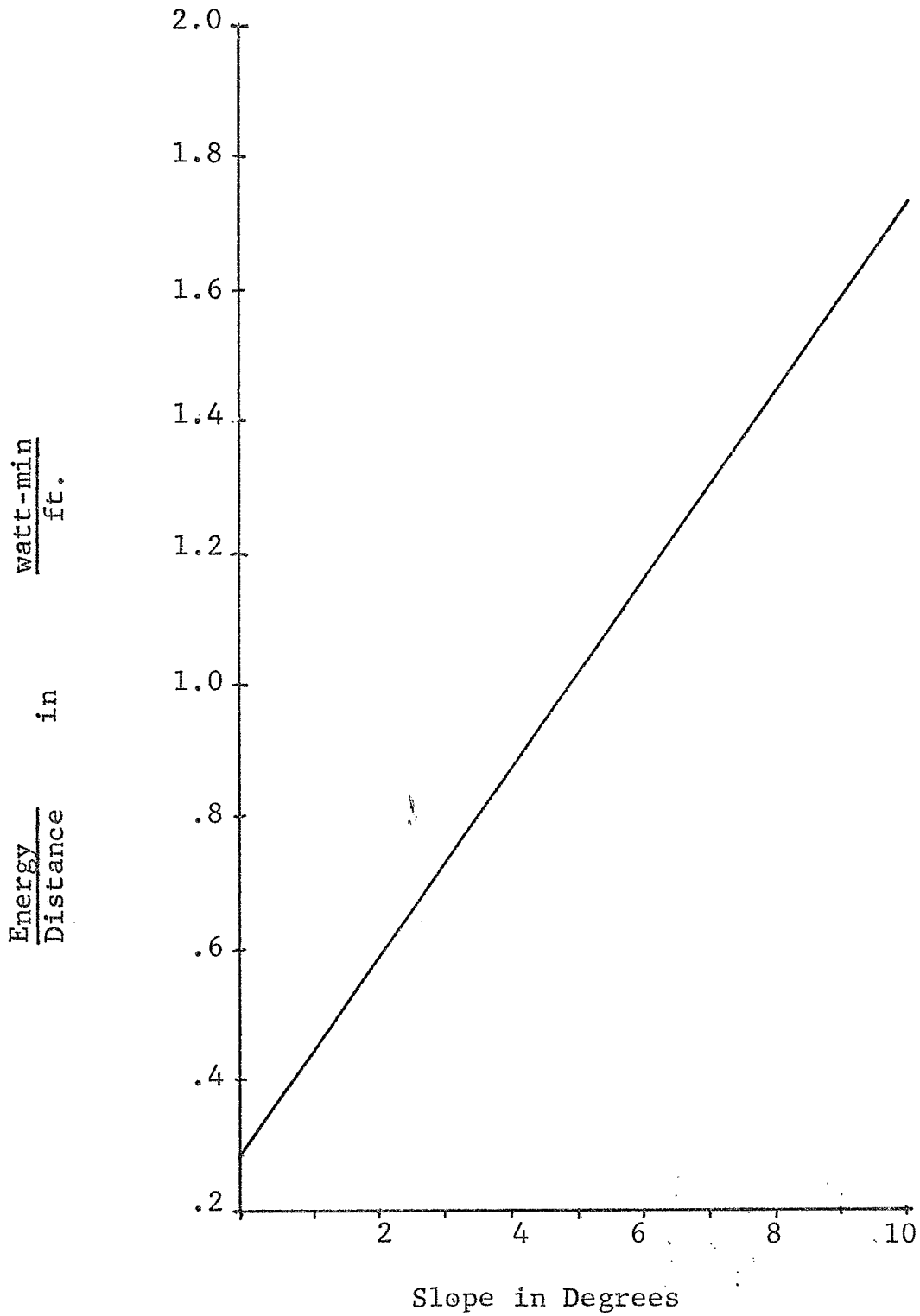


FIGURE 20b. Energy Requirements for Propulsion of the Vehicle.

the vehicle. Plans now call for a dual mode power supply system. The major part of the power load is to be handled by a radioactive thermal generator (RTG). For periods of peak power requirements, such as climbing steep slopes, batteries would be used to supply the extra power. The batteries would then be recharged by the RTG. It is not unreasonable to think that regenerative braking would also be used to recharge the batteries while traveling on downslopes.

The peak power was considered for a time to be the limiting factor. But it is assumed, that in cases of emergencies, that the vehicle has the ability to climb at least a 25 degree slope. To do so, that much power must be available. The present terrain modeling process defines any region with a gradient of over 10 degrees as a gradient obstacle. Therefore, for the purposes of path selection, it is not the power that is the important factor but the length of time the power is required; that is, energy. Also, the power supplied by the RTG is considered to be "free" in that it is nondepletable, constant, power supply. In conclusion, it is the energy drain of the batteries that is the important factor to consider.

As a performance index, the actual value of the energy drain on the batteries is an easy factor to use. For a given RTG level, the graph of energy per distance vs. slope can be modified to be the energy of the battery per distance vs. slope. From this and the path generated by a path-selection

algorithm on a sample terrain, the total energy drain of the batteries can be found. This value can then be used to compare the algorithm to others used on the same sample terrain to find out which does the best job of minimizing the total battery drain.

A set of meaningful sample terrains needs to be developed for the evaluation of algorithms with respect to energy. This has not been done. The major obstacle to doing this is the inability to simulate three dimensional terrain on the digital computer. This capability is a must before such work could be attempted.

Caution must be used when comparing algorithms because the fact that one path-selection algorithm produces a path with a lower energy drain does not automatically indicate that that algorithm is indeed the best. A path-selection process needs to make a trade off between the energy of the battery that is used and the distance that the vehicle will travel towards the target. For example, a path-selection algorithm that picks a path with zero battery drain whenever possible would be far from the most desirable. A path leading to the target with zero battery drain might not exist. Paths with zero battery drain could lead the vehicle away from the target. Even if such a zero energy path did exist, the length of time required to travel such a path might make it less desirable than others available. In the evaluation of various algorithms this trade

off must be kept in mind and a way of judging this trade off must be developed. This matter is further discussed in section IV where a new path-selection algorithm is presented that automatically makes this trade off between the energy and the distance traveled toward the target.

Implications for Future Algorithms

Once it was determined that the energy used by the vehicle was a very important factor, a rather fundamental question had to be answered. Is it possible for the two dimensional path-selection algorithms now in existence, or any two dimensional algorithms, to take this important factor into consideration when making its selection?

The present path-selection algorithms use the information from the terrain modeling process as a two dimensional, go, no-go map. While some energy information is contained in this type of map, in that any region having a gradient of greater than 10 degrees is labeled a gradient obstacle, this is not enough. If the vehicle has an RTG power output of 300 watts and is to maintain a constant speed of 3 mph, the break point between "free" power from the RTG and "costly" power from the batteries is about 4 degrees. The actual value of this break point varies directly with the RTG power output and inversely with the vehicle speed. However, the 300 watts of RTG power is considered a maximum, and the slowing of the vehicle to

reduce the power required is costly in terms of time, and therefore the break point would be expected to be in the under 10 degree, free region. The two dimensional path-selection algorithms use no slope information under 10 degrees so they don't consider the most fundamental information necessary to make the best selection with respect to energy.

A simple example will show the inadequacy of the present algorithms. Fig.21 shows a simple terrain and two possible paths. The path to the right of the obstacle involves the climbing of considerably higher slopes than the path to the left of the obstacle. One of the two dimensional algorithms would pick path 1 to follow because it maximizes the distance traveled toward the target. Algorithms need to be developed that will include slope information throughout the free regions of the terrain map so that a path such as path 2 would be selected. Such a path would be more desirable than path 1, provided it used considerably less battery energy, because the distance traveled toward the target is only slightly less than for path 1. Again, a decision level must be set up as to make the trade off between energy and distance traveled.

The example shows that the two dimensional algorithms are not capable of making the proper selections with respect to energy. This will be demonstrated to greater detail again in part IV. Three dimensional path-selection algorithms are

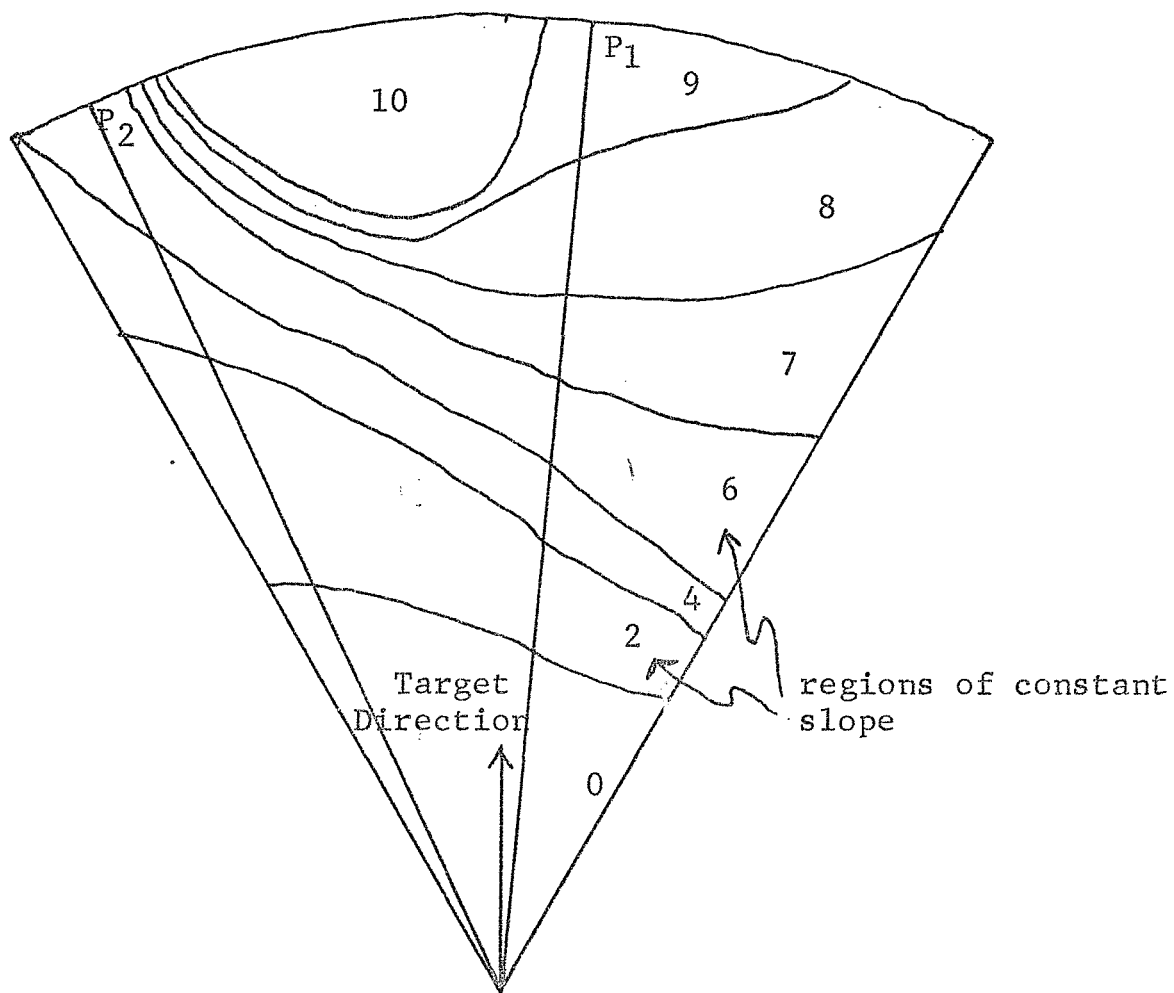


FIGURE 21. Terrain and Possible Paths (showing importance of energy considerations).

definitely needed that will consider all slope information. This will also make necessary the modification of the terrain modeling section so that the necessary information is available for the path-selection algorithm to use.

D. Summary

Two performance indexes have been formulated. Each of these is related to one of the important parameters of the over-all system. The average danger index is a measure of how close the vehicle would travel to obstacles and is related to the safety of the vehicle. The total battery energy used on a path is a direct measure of that important parameter. It has been demonstrated how each of these indexes can be used in the evaluation of different path-selection algorithms.

The implications that the work on the evaluation of algorithms has had to the writing of future algorithms has been discussed. These ideas have been put to use in the formulation of a three dimensional path-selection algorithm that takes into consideration both the safety of the vehicle and the energy-distance trade-off. This algorithm is presented in detail in the last section of the report.

It is important to use three dimensional terrain whether it be for the evaluation of existing algorithms or as an aid in the formulation and testing of new three dimensional algorithms that are needed. At present, there is no capability of simulating three dimensional terrain on the digital computer.

The capability is a must before much more work can be done in either of these areas.

IV. TOTAL PACKAGE FOR AUTOMATIC ROVING CAPABILITY

A. Introduction

Considerable work has been done in the areas of terrain modeling and automatic path-selection algorithm formulation and evaluation. However, this work has never been combined to produce an integrated, total system that would accept terrain data as the input and give heading commands as the output.

Section III showed the need for the development of new, three dimensional, path-selection algorithms that would make a path selection with respect to the safety of the vehicle and the energy drain of the vehicle's batteries on the path. Such an algorithm is developed in this section. For simulation, it was decided to integrate this new path-selection algorithm with the terrain modeling process discussed in Section II. This would, for the first time, show the feasibility of a complete system.

B. 'Cost' Considerations and Interfacing

In order to formulate a new path-selection algorithm the important costs had to be determined. This subject was discussed in detail in Section III. To summarize the findings of that section, the important factors to be considered are:

1. total energy drain of the batteries
2. maximization of the distance traveled toward the target
3. safety of the vehicle when traveling near obstacles

In the process of selecting a path, the path-selection algorithm will attempt a suboptimization of the available paths with respect to the above factors in its selection of a path.

To implement the algorithm, information about the energy required to propel the vehicle is needed. The vehicle design presently being considered has a dual-mode power supply. Part of the power will be supplied by a radioactive thermal generator (RTG). Its output rate would be limited, but its power can be considered "free" in that it is a constant power source, not subject to drain over the mission life-time. The rest of the power would be obtained from a battery system whose output would be considered costly in view of the fact that recharging of the batteries limits operating time and is never 100% efficient or indefinitely repeatable. A graph of the energy of the batteries needed to propel the vehicle was derived from the following assumptions.

1. constant vehicle speed of 3 mph.
2. an RTG power level of 300 watts.
3. a drive-train efficiency of 70%.
4. absence of regenerative braking
5. that only the change in potential energy need be considered in calculating power output on a slope.

6. use of a 2 degree slope as level ground to account for frictional losses.
7. vehicle Earth weight of 1000 pounds.

From these assumptions, the equations for the power (P) and energy (E) required by the vehicle to climb a given slope of λ degrees are

$$P = 2.21 \times 10^3 \sin (\lambda + 2^\circ) \text{ watts}$$

$$E = 8.38 \times D \times \sin (\lambda + 2^\circ) \text{ watt-min.}$$

The graphs of these equations are shown in Figs. 20a and b. As already noted, it is only the energy that is used from the batteries that is a costly factor. The assumed output of 300 watts from the RTG means that climbing slopes up to about 4 degrees is not costly at a speed of 3 mph. The graphs of Fig. 20 can then be modified to be an "energy of the batteries per distance vs. slope" graph that is shown in Fig. 22. This is the graph that is needed for the calculations in the new path-selection algorithm.

To calculate the energy of the battery that would be used along a given path, the terrain modeling process must be modified to do the following iterative calculations. These calculations approximate the actual energy expended on an "n" point path. Adjacent points along the path are separated by distances

D_i where $1 \leq i \leq n-1$. First,

(see Section II)

$$G_i = \sqrt{(S_T)^2 + (S_c)^2}$$

from Fig. 22,

$$\left(\frac{E_{\text{Batt}}}{D}\right)_i = \begin{cases} 0 & \text{if } G_i \leq \tan 4^\circ = .06993 \\ 8.29 G_i - 0.58 & \text{if } G_i > .06993 \end{cases}$$

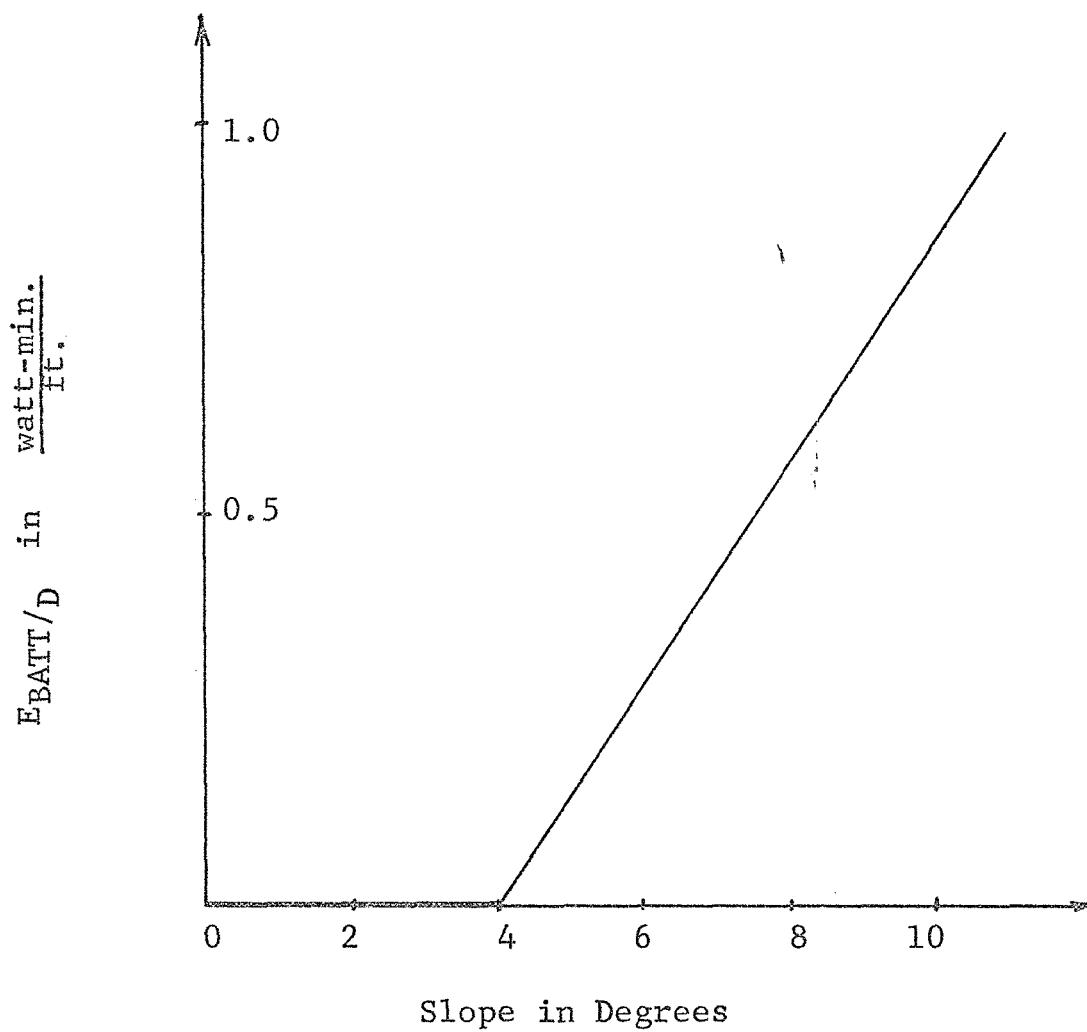


FIGURE 22. Battery Energy Drain Per Distance vs. Slope

then
$$E_{BATT} = \sum_{i=1}^{n-1} \left(\frac{E_{BATT}}{D} \right)_i (D_i),$$

and the battery drain (E_{BATT}) on the path has been calculated. These calculations can be done simultaneously with the obstacle calculations in the terrain modeling section of the system.

An important part of the path-selection algorithm is the handling of the energy-distance trade-off. Having no empirical information as to what decisions would be best, a logical approach would be heuristic, where decision levels are determined from the examination of numerous cases. For example, it could be demanded that a path using 1/2 the total energy of another path be at least 2/3 as long before that path would be selected.

Calling the longer path P_1 and the shorter path P_2 , the decision level K_B is given by

$$K_B = \frac{D_{T2} E_1}{D_{T1} E_2}$$

Where D_{T1} and D_{T2} are the distance traveled toward the target and E_1 and E_2 are the energy costs on the respective paths.

This definition applies only to paths that are free of gradient and unknown region obstacles.

In the definition of the decision level K_B the energy cost term E_2 can not be allowed to become zero. Therefore, the energy cost is defined to be the sum of the energy expended by

the battery and a second term that is dependent only on the path length. This would correspond to the idea that even if the battery energy used on a path were zero that there is still some cost involved with traveling that path. The energy cost is then defined by:

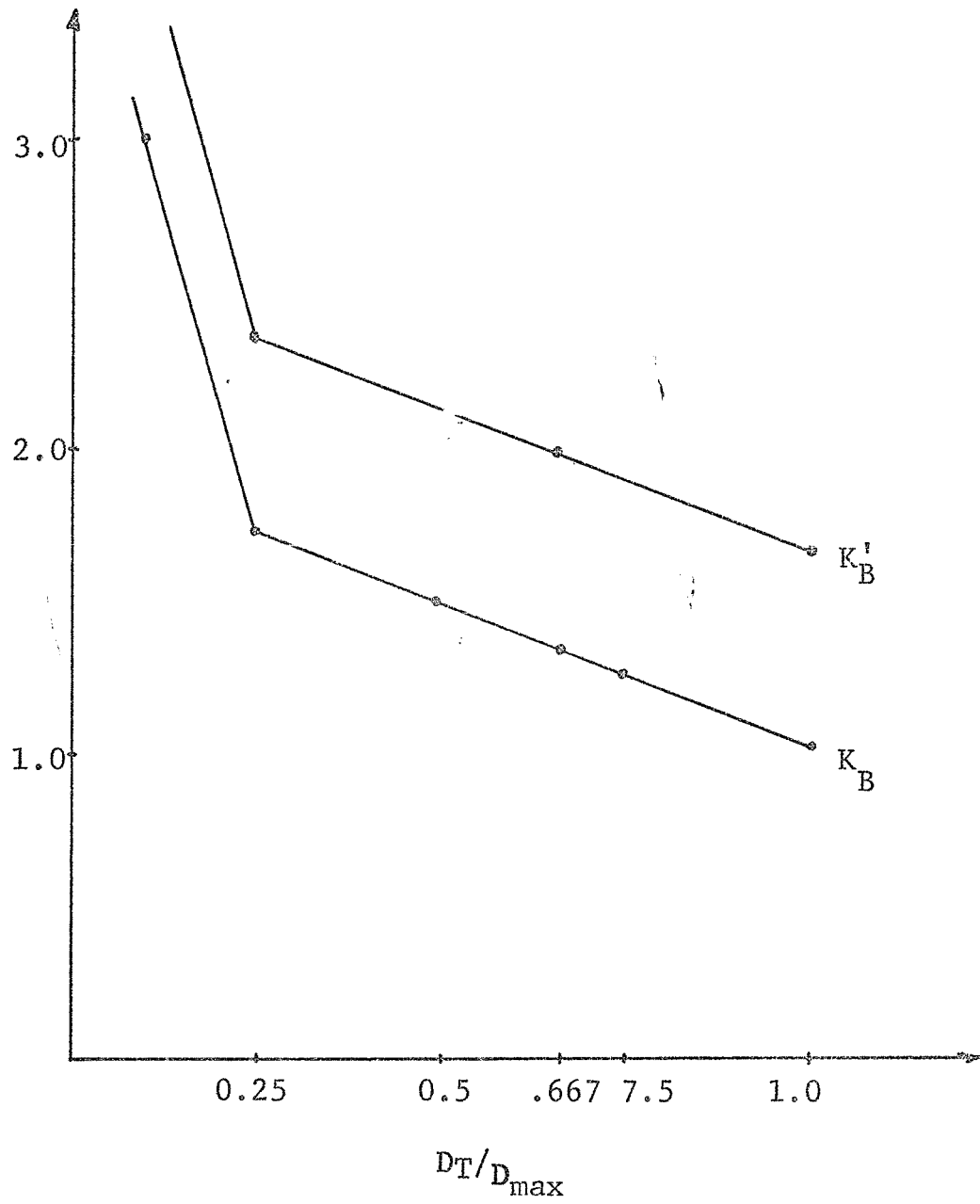
$$E_c = E_{BATT} + 0.05(D_{TOT})$$

Let D_{max} be the distance toward the target of the path to be used as a standard and D_T the distance towards the target achieved by traveling any other path. By considering a number of examples like the one described above, a graph for the definition of K_B as a function of $\frac{D_T}{D_{max}}$ can be generated. This graph is shown in Fig. 23. It should be noted that this defining graph for K_B is not unique but that any similar definition could be used and the general operation of the algorithm would not be affected.

The steeper slope in the graph for K_B for small values of D_T/D_{max} reflects the fact that short paths are highly undesirable. This definition of K_B deals with the trade-off between energy and distance along clear paths. The problems concerned with the safety of the vehicle will have to be dealt with.

Having taken care of the energy-distance trade-off, attention is turned toward safety considerations. The following alternatives were identified:

FIGURE 23. Definition of Trade-off Levels



- 1) reject any path toward a gradient obstacle or unknown region
- 2) reject any path next to a gradient obstacle or an unknown region
- 3) use guard bands around obstacles and forbid travel within these areas
- 4) increase K_B for any path in proximity of a gradient obstacle or unknown region

When the vehicle travels a path leading toward an unknown region there is the question of what type of terrain is contained in that region. Because of the possibility that the unknown region actually contains impassable terrain, a path leading to such a region should be penalized in some way compared to a path that is free. One way of doing this is to assign a higher value of K_B to a path that approaches an unknown region. For example, if the ratio of D_T/D_{max} is $2/3$, let the value of K_B be 2, rather than $4/3$, if the path leads to an unknown region. This modified K_B' is also shown in Fig. 23.

C. A Path-Selection Algorithm

Having calculated a breakeven point, or decision level, for a path in terms of the energy cost-distance trade-off, it is logical to describe the path by its performance relative to its break even point. Let all paths be compared to the one that gives the greatest distance traveled toward the target, D_{max} with energy cost E_{max} . Then the graph for

K_B assigns to each path its own characteristic break even point dependent on the ratio D_T/D_{max} . This represents the maximum energy cost on the path for which that path would be more desirable than the path of length D_{max} .

An actual measure of the quality of a path is K , where K is given by:

$$K = \frac{D_T E_{MAX}}{D_{MAX} E_C} .$$

The ratio K/K_B then gives a measure of how well each path compares with its own break even point. If this ratio is greater than 1 it indicates that the path is better than the path that maximizes the distance traveled toward the target, the one defined as D_{max} . In other words, the reduction in the energy cost is large enough to offset the decrease in the distance traveled toward the target.

Of all paths considered, the path-selection algorithm should pick the one with the maximum value of K/K_B . In terms of the major costs this path out performs all the others and is therefore the most desirable path.

D. Simulation

The simulation of the total system with terrain data as input and a selected path as the output was performed making the following assumptions:

1. only azimuth lines were considered as possible paths

2. azimuths ending in gradient obstacles were not considered.
3. azimuths on either side of a gradient obstacles or unknown region were not considered.
4. gradient obstacle is a region with a 10 degree gradient or greater.
5. guard bands of width L were placed on maximum range obstacles, where $L = (0.08) \times R_{\text{obst}}$, and R_{obst} is range to the obstacle.
6. use K_B^1 for an azimuth ending in an unknown region.
7. guard bands of width L' were placed on gradient obstacles, where $L' = (0.10) \times R_{\text{obst}}$.
8. $D_T = D_{\text{TOT}} \cdot \cos \Theta$ where D_{TOT} is the total azimuth path length.

The terrain modeling process was modified to output the necessary battery drain, or energy cost, information to the path-selection section. This was the only modification necessary to integrate the two sections into one working unit. Fig. 24 shows a simplified block diagram of the total system.

The first terrain that was discussed in Section I was used for the simulation. Table 3 presents the data used and shows the step by step calculations for determining K/K_B .

Figure 25 is a graph of the ratio K/K_B as a function of the azimuths. Finding the maximum ratio, the path-selection

FIGURE 24. Block Diagram of Total Package

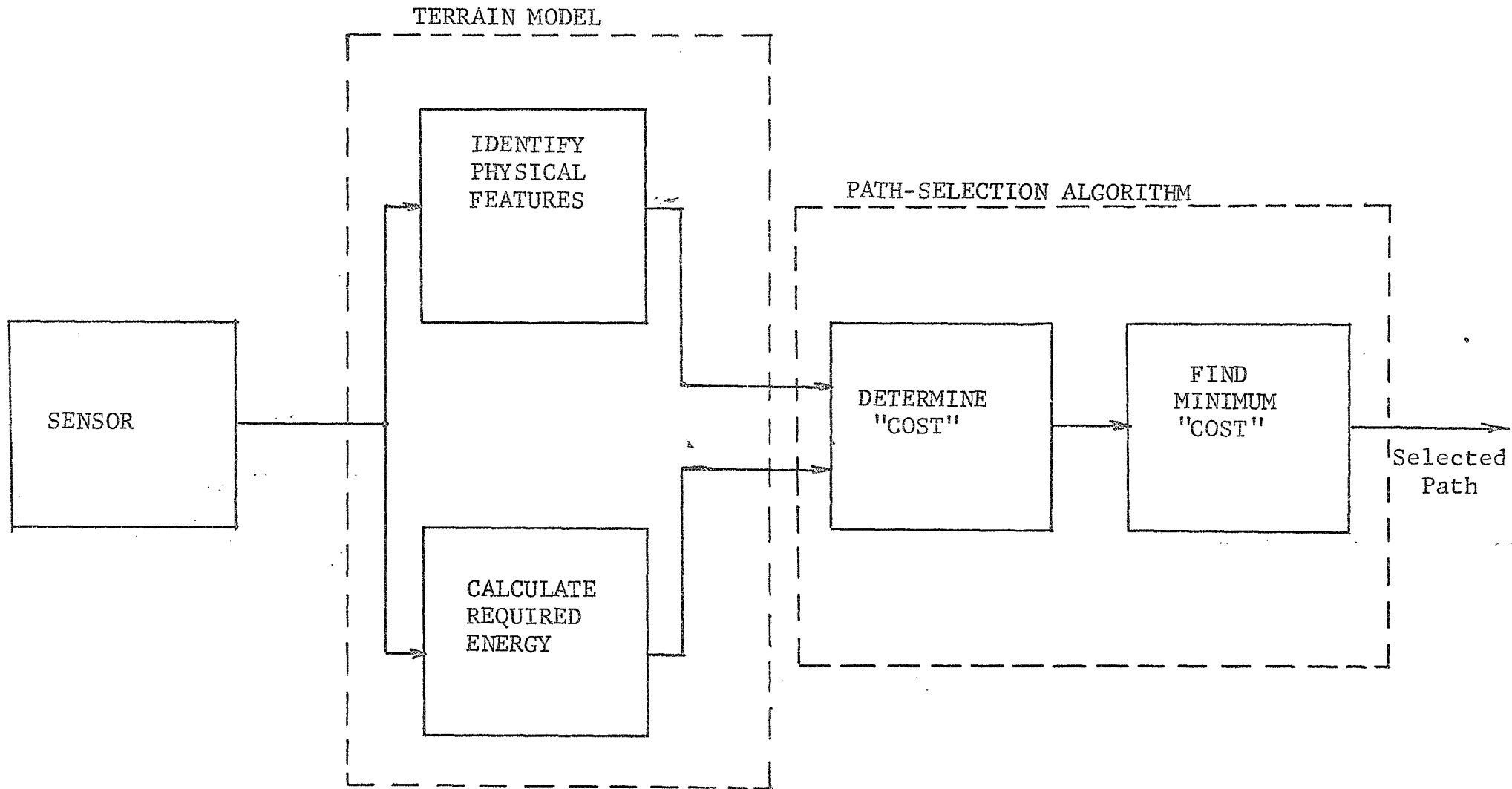


TABLE 3

Data and Calculations for Simulation of Total Package

Azimuth (degrees)	Robst (feet)	DT (feet)	EBATT (watt.min.)	E_c (watt.min.)	K_B	K	K/K_B
-45	1535	1085	54.8	131.5	1.28	2.19	1.71
-40	1555	1190	79.1	156.9	1.18	2.07	1.75
-35	1530	1255	134.4	210.9	1.13	1.64	1.45
-30	1410	1220	142.1	213.1	1.16	1.56	1.35
-25	1500	1360	249.7	324.7	1.07	1.14	1.09
-20	1500	1410	314.1	389.1	1.03	.99	.96
-15	1500	1450*	304.9	379.9	1.00	1.05	1.05
-10	1455	1430	313.8	396.5*	1.01	.99	.98
- 5	1015						0
0	1115						0
5	1100						0
10	1090						0
15	1160						0
20	1260						0
25	1530	1380	208.3	284.8	1.05	1.33	1.26
30	1500	1300	49.85	124.9	1.15	2.72	2.36
35	1550	1270	19.50	97	1.12	3.58	3.20
40	1480	1130	0	74	1.22	4.20	3.44
45	1500	1060	0	75	1.27	3.86	3.04

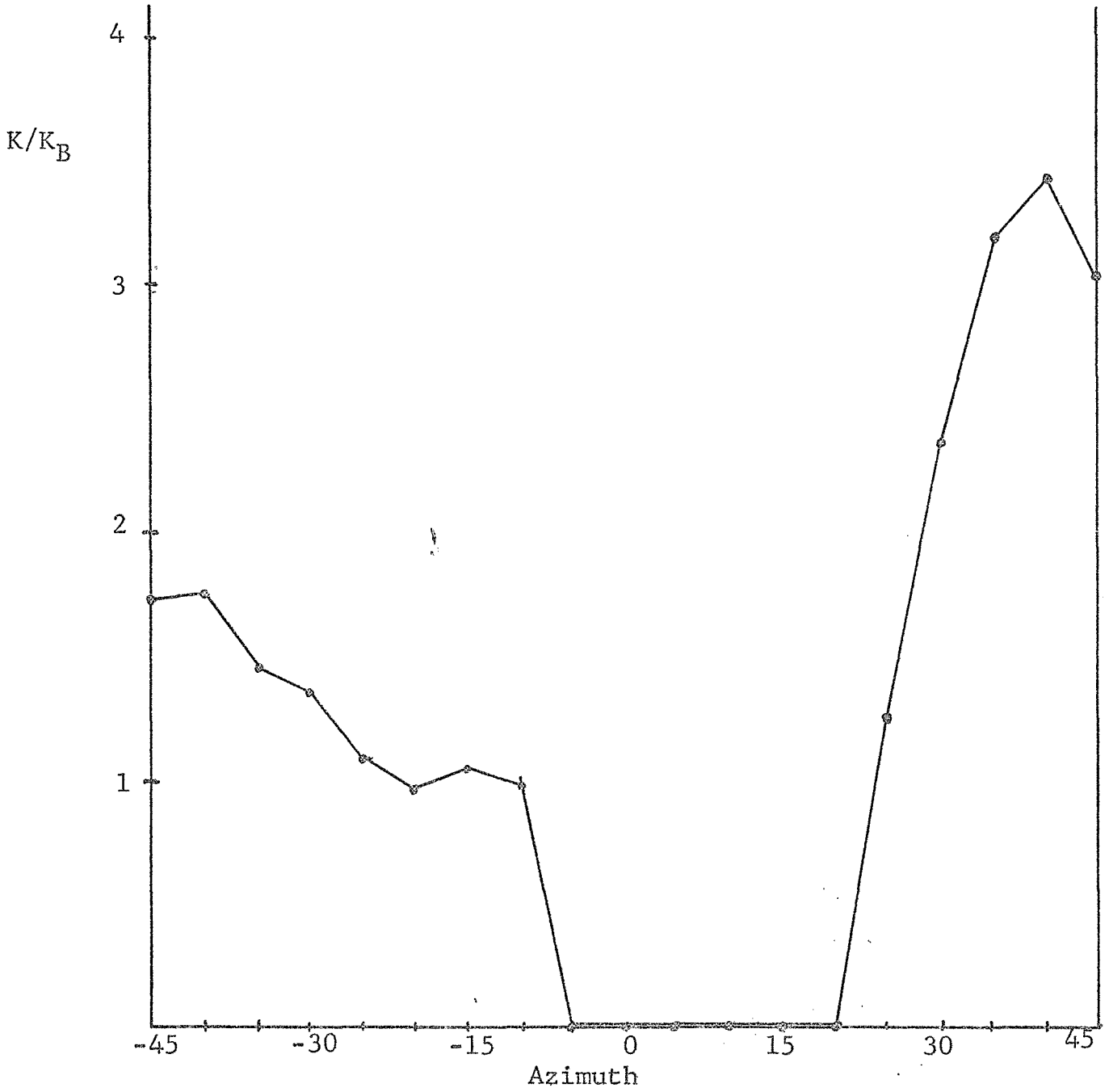


FIGURE 25. K/K_B vs. Azimuth Path

algorithm would pick azimuth (+40°).

The paths to the far right on the sample terrain are intuitively the "best" as they use the smallest amount of battery energy. Of the group of flow-energy azimuths, the path-selection algorithm chose an azimuth that resulted in zero energy drain of the batteries. As a second choice, it preferred to spend a small amount of battery energy in order to gain a greater distance towards the target, i.e., azimuth (+35°) was chosen over azimuth (+45°).

It is realized that the path-selection algorithm presented is not useful for evaluating paths which vary from the target direction by 90° or more. In the case where all paths in a +85° scan of the target direction are blocked, a possible solution would be to assume a new target direction until this obstacle region is safely skirted and then to recalculate the actual target direction and resume normal operation.

E. Summary

A major achievement of this section was the demonstration of the capability to write a path-selection algorithm that considered all important cost criteria of a path. No claim is made as to the efficiency of this algorithm compared with some theoretical optimal method. The trade-off levels between costs were set intuitively by the authors and these levels can be easily changed to alter the response of the algorithm.

It was possible and relatively simple to modify the terrain model discussion Section II in order to complete the integration process. Most of the additional information required of the terrain model was already available as a product of the obstacle calculation procedure.

The simulation in this section demonstrates, for the first time, that the creation of a total package is feasible.

V. CONCLUSION

Considerable gains have been made toward the eventual creation of an automatic roving capability for an unmanned Martian exploratory vehicle. The effect of the operating parameters of an ideal errorless terrain sensor upon the quality of incoming terrain data was determined. Restrictions on sensing parameters were then obtained, and a suggested set of parameters was listed. A 3-point planar approximation to the actual terrain was generated by appropriate processing of the sensor data. Simulation demonstrated that the process closely approximated major terrain features.

Path-selection algorithm evaluation was studied for the purpose of evaluating existing algorithms and as a guide to formulating future algorithms. Safety and energy considerations were determined to be the important areas of concern following an examination of the terrain modeling process and vehicle design. Performance indexes were then formulated to assign a

quantitative measure to algorithm performance.

The work in path-selection algorithm evaluation demonstrated that there were no existing algorithms that considered all major cost factors related to vehicle travel. Consequently, an algorithm was formulated that automatically made the energy-distance trade-off while guarding the safety of the vehicle. The algorithm and terrain modeling process were then interfaced to form a complete operating system.

The logical next step in the development of a roving capability is to remove the assumption of an ideal sensor. Using a sensor with errors in sensing parameters (θ, β) and range calculation, the resultant errors in the terrain model should be examined. Then, the effect of these errors on terrain definition, major feature detection and the operation of a path-selection algorithm can be determined.

REFERENCES

1. Mancini, R.J., "Terrain Modeling for Surface Vehicle Guidance", RPI Technical Report MP-11, NASA Grant NGL 33-018-091, August 1969.
2. Elion, H.A., Laser Systems and Applications, Pergamon Press, 1967.
3. Carroll, Story of the Laser, Dutton & Co., 1964.
4. Marshall, R.R., "Terrain Model of Mars for Roving Vehicle Motion-Control Evaluation", Space Programs Summary 37-55, Vol. III, JPL, Feb. 28, 1969.
5. "Science", Oct. 3, 1969, No. 3901, p. 49.
6. Lallman, F., "Automatic Path Selection", Technical Report V of Progress Report, "Analysis and Design of a Capsule Landing System and Surface Vehicle Control System for Mars Exploration", By P.K. Lashmet, et.al., NASA Grant NGL 33-018-091, RPI, June 1968.
7. Lim, L.Y., "A Pathfinding Algorithm for a Myopic Robot", Technical Report 32-1288, Jet Propulsion Laboratory, August 1, 1968.